

<b>CHAPTER 5</b>	<b>TYPHOON WINDS</b>
<b>5.1</b>	<b>Introduction ^</b>
<b>5.2</b>	<b>Measurement of Wind Speed ^</b>
<b>5.2.1</b>	<b>Anemometry ^</b>
<b>5.2.2</b>	<b>Beaufort Forces ^</b>
<b>5.2.3</b>	<b>Average Speeds and Gusts ^</b>
<b>5.3</b>	<b>Low-level Wind Fields ^</b>
<b>5.3.1</b>	<b>Radial Variation of Wind Speed ^</b>
<b>5.3.2</b>	<b>The 300 m Wind Field ^</b>
<b>5.3.3</b>	<b>The Surface Wind Field ^</b>
<b>5.4</b>	<b>Three-dimensional Structure ^</b>
<b>5.4.1</b>	<b>Upper Level Wind Field ^</b>
<b>5.4.2</b>	<b>The Friction Layer ^</b>
<b>5.5</b>	<b>Maximum Winds ^</b>
<b>5.5.1</b>	<b>The Maximum Wind Region ^</b>
<b>5.5.2</b>	<b>Central Pressure/ Maximum Wind ^ Relationships ^</b>
<b>5.5.3</b>	<b>Extreme Wind Observations ^</b>
<b>5.5.4</b>	<b>Statistical Estimation of Extreme Winds ^</b>
<b>5.5.5</b>	<b>Extreme Wind Estimates ^</b>
<b>5.6</b>	
<b>5.7</b>	
<b>5.8</b>	<b>Winds and Engineering Design</b>
<b>5.8.1</b>	<b>Winds and Buildings</b>
<b>5.8.2</b>	<b>The Design Wind Speed</b>
<b>5.8.2.1</b>	<b>Selection of Averaging Period</b>
<b>5.8.2.2</b>	<b>Selection of Return Period</b>
<b>5.8.2.3</b>	<b>Determination of Wind Loading</b>
<b>5.8.3</b>	<b>Measurements at Full-scale</b>
<b>5.8.4</b>	<b>Windows</b>
<b>5.8.5</b>	<b>Wind and People</b>
<b>5.8.5.1</b>	<b>Body Forces</b>
<b>5.8.5.2</b>	<b>Variation Tolerance</b>
<b>5.8.5.3</b>	<b>“Skinburn” and Windchill</b>

## 5.1 Introduction

In general, tropical-cyclone-winds do not directly cause as much damage or loss of life as wind-driven storm-surge and waves or heavy rainfall. Nevertheless, they are a great destructive force, as was tragically illustrated by the devastation of much of Darwin by cyclone Tracey on Christmas day 1974 (Figs. 5.1(1) to 5.1(4)). At sea, and in areas secure from storm surge, landslips and swollen rivers, the threat of winds is paramount.

The force on an object due to the wind is proportional to the latter's kinetic energy, that is to the product of the square of the wind speed and the air density. The force also depends on the shape, porosity and surface roughness of the object. Structures need to be both well designed and well constructed to withstand sustained winds in excess of 60 m/s; at this speed the forces involved will be 12.5 times greater than in gale force winds of 17 m/s. Fortunately, the area covered by winds of hurricane force in a tropical cyclone is, on average, only about 13% of the area covered by winds of gale force or more (Fig. 5.3.1(1)). Consequently, it can happen that one town can be completely devastated by wind while others nearby suffer little damage. It is for the same reason that the frequency with which sustained hurricane force winds strike a given community or installation is low when compared to the frequency of tropical cyclone gales.

In the last two decades many papers have been written by meteorologists and engineers on the extreme surface wind speeds in tropical cyclones, but the subject is plagued by many difficulties and pitfalls. There are problems associated with the response of anemometers to extreme and gusty winds and others related to the exposure of the instruments. Most anemometers fail before the peak wind speeds are attained and, because the wind speed varies around the eye of an advancing typhoon (Fig. 5.3.2(1)), it is not usually possible to be sure that surviving instruments experienced the



Fig. 5.1(i). Darwin homes destroyed by Tracy on Christmas day 1974.  
(Photo by courtesy



Fig. 5. 1(2) Darwin houses with roof and upper storeys missing.  
(Photo by Andrew Fraser)



Part of the damage at Darwin Airport.

Fig. 5. 1, (3) Blown away car, airplane and airplane tail at Darwin airport  
Note defoliated trees. (Photo by courtesy)

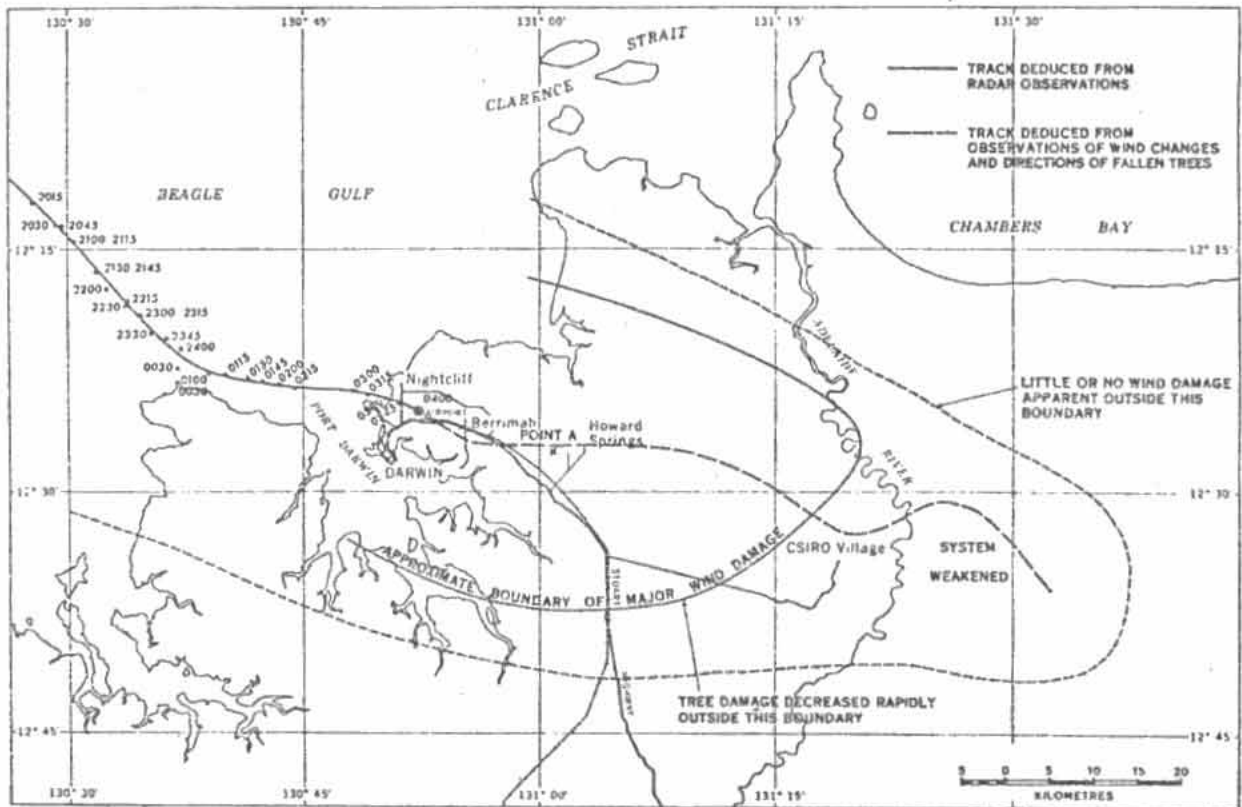


Fig. 5.1.(4). The final section of cyclone Tracy's (1974) track across Darwin showing the pattern of wind damage as determined from aerial surveys. Major wind damage was confined to a radius of about 17 km from the cyclone centre and extended about 50 km inland. (From the Australian Bureau of Meteorology 1977.)

strongest winds. Thus, the strongest winds in the most intense tropical cyclones have never been measured. However, it is likely that once every few years a typhoon in the favoured area to the east of the Philippines island of ~~Lu~~ Luzon will generate gusts of up to 125m/s at a height of a hundred metres or so, and speeds of 90 m/s may be sustained over a few hours.

When describing, using or comparing wind speeds it is necessary to know the averaging periods to which they refer. Wind averaged over one hour, ten minutes, two minutes, one minute, three seconds and instantaneous peak gust speeds are in widespread use. The "fastest mile" of wind is also in use in the U.S.A. In general, for a given storm these various wind speeds will differ from one another (Bell 1961). In two 1974 research papers from authoritative national meteorological services not only have wind speeds of different averaging periods been incorporated into a supposed homogeneous set but so also have wind speeds in different units. W.M.O. Technical Regulation (1980) 10.2.2.1 requires that wind speeds for shipping should be given in m/s - the primary S.I unit - or knots. But, nevertheless, it is remarkable that a navigator crossing the Pacific Ocean in 1980 should receive reports on tropical-cyclone wind speeds in statute miles per hour in the U.S.A. - and in technical reports there - in knots from the U.S. Joint Typhoon Warning Centre at Guam, kilometers per hour from the Philippines and Australia and in metres per second from China, North Korea and Vietnam. So that, in the Pacific, the inferior limit for hurricane force winds would then be 33 m/s, 64 kn, 76 mph or 119 km/h and it could refer to a one minute, a ten minute or a one hour average according to the source of the information!

This chapter presents a discussion on the problems and limitations of wind speed measurements in tropical cyclone conditions ~~and~~ and this is followed by a description of the major features of the low-level wind field and three-dimensional structure of tropical cyclones. A discussion of the observed and estimated maximum winds in tropical cyclones, together

with a comprehensive overview of the use of winds in engineering design, then complete the chapter.

### 5.2.1 Anemometry

The velocity of the wind at a place varies with time and with height above the earth's surface. If surface wind measurements are to be comparable with one another it is necessary to specify a height above open ground at which the measurements should be made and the period over which the readings should be averaged. Current (1980) W.M.O. Technical Regulations [A.1.2] 4.7 specifies that the surface wind is the horizontal wind at 10 m above the sea, or over open flat ground, averaged over a period of about 10 minutes. It is often difficult to obtain open sites where the wind is free from the effects of trees, buildings or high ground. Lighthouses, although over open sea are usually higher than 10 m and the placing an anemometer on them below the top can result in the house shielding the instrument for winds from some directions and accelerating the winds from some other directions. An anemometer 10 m above the general level of the earth's surface but on top of a building, small island or mound will not measure the free wind; the deformation of the wind flow over or around the supporting building or elevated ground will affect the readings of the anemometer in a complicated way which may vary with atmospheric stability and the direction speed and gustiness of the wind. Similar considerations apply to an anemometer 10 m above ground which is not flat for radii of a few kilometers.

In addition to the siting problems there are uncertainties in the performance of the instruments themselves in the extreme and very turbulent winds found in mature typhoons. Anyone using typhoon wind records for meteorological or engineering purpose should thus take care to incorporate the properties of the anemometers involved. The theoretical aspects of the response of anemometers are examined in a number of papers (e.g. MacCready

1966, Mazzarella 1972). In its simplest form the problem is that standard cup and propeller type anemometers accelerate more quickly in an increasing wind than they decelerate in a falling wind, so that, in a fluctuating wind, such anemometers record a mean wind speed higher than the true mean. Experimental tests and theoretical studies on cup anemometers have variously put the overestimation of the mean at between 1 and 30% depending on wind speed, the anemometer design and the frequency and amplitude of the wind fluctuations. The WMO Guide to Instruments and Observing Practices (4th Edition) puts the overestimate at "as much as 15%, and experiments in which the readings of cup anemometers were compared with those from a sonic anemometer (Isumi and Barad 1970) indicate overestimates of 8 to 16%. However, these comparisons were not made in winds of hurricane force. Comparisons of the corrected readings of a Dines pressure tube anemometer and a good 3-cup anemometer (British) Meteorological Office Mk II) have been made in some typhoons at Hong Kong. As shown in Fig 5.2(1) the ten <sup>MINUTE</sup> mean winds are in good agreement up to about 30 m/s but at higher speeds the cup anemometer tends to read higher than the Dines by an amount which reaches about 20% at 40 m/s; a similar bias holds for 60 minute mean winds. The instruments, were located on an offshore island (Waglan) at a height of 74.7 m above m.s.l where the flow is less turbulent than at 10 m (Chen 1975), thus greater differences might be found at lower levels. Note, however, that peak gust speeds recorded by the cup and the Dines anemometers are of comparable magnitude; this result should be expected because tests show that, providing the Dines tubes are not too long or too narrow, both instruments take less than 2 s to register 90% of a sudden increase in winds of gale force or more (Meteorological Office 1956, Sanuki 1952).

Standard propeller anemometers (aerovane) suffer from the same kind of error as do cup anemometers, but in addition there are errors due to the axis of the propeller not being correctly aligned with the wind flow. Sudden changes of direction in hurricane force gusts probably contribute to the high frequency with which these anemometers fail in winds of 60 m/s or so. However, strengthened versions are now available.

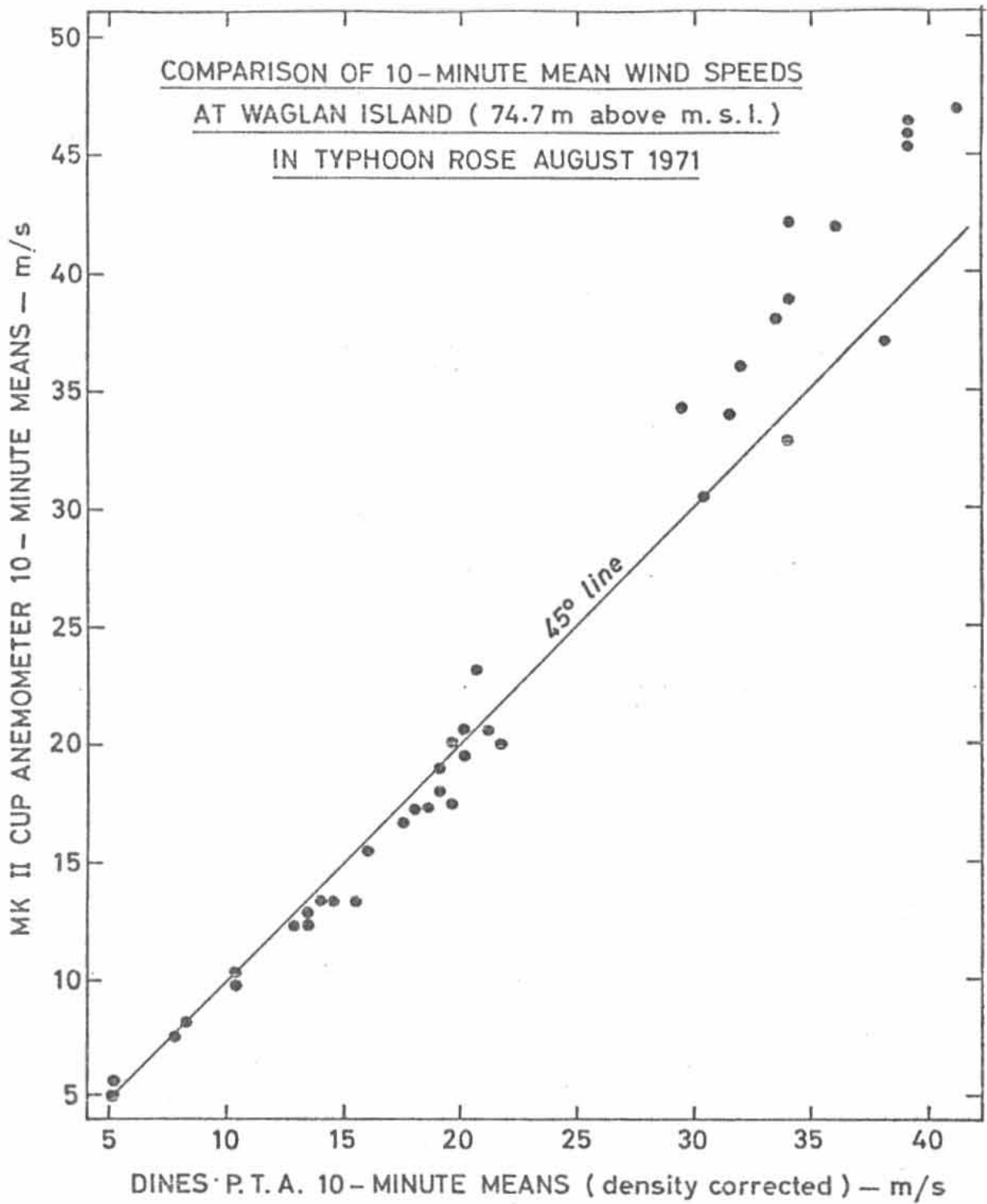


Fig. 5.2.(1) Comparison of 10-minute means measured by well exposed cup and pressure tube anemometers mounted on the same mast.

The principle of the method of operation of a Dines pressure-tube anemometer is that when a wind blows into the mouth of a tube it causes a pressure rise in the tube whereas a current blowing across the mouth causes a reduction in pressure. The difference between these two pressures increases with wind speed and is used to raise a floating piston (the float) to indicate speed. An advantage of this type of instrument is that its calibration can readily be checked. The indicated speeds ( $v_i$ ) need to be corrected for departure of the density of air from standard using the relationship.

$$\text{corrected speed} = v_i \left[ \frac{\text{standard density}}{\text{station density}} \right]^{0.5} = v_i \cdot 1.876 \left[ \frac{\text{stn. temp (K)}}{\text{stn. press (mb)}} \right]^{0.5} \quad (5.2(1))$$

For example, the correction to the indicated winds in a storm with station pressure between 910 and 990 mb amounts to about +5%.

Middleton (194<sup>1</sup>) suggested that the float of the Dines anemometer might rise more readily than it falls so leading to an overestimate of average wind speeds. But Fig. 5.2(1) suggests that this effect, if it exists, must be small in comparison with the overreading of cup anemometers.

In extremely turbulent conditions, such as are found downwind of high-rise buildings in very strong winds, the Dines wind vane may find itself momentarily at a significant angle to the wind flow so that the positive air pressure is reduced or even replaced by suction. The Dines float then hits the bottom stops. This effect can be seen in the Royal Observatory record for typhoon Wanda in Fig. 5.2(2). After the wind direction change at 9 a.m. frequent bottoming of the pen occurred as the anemometer was then in turbulent eddies to the lee of a high building. Some of this bottoming would have been due to misalignment of the anemometer vane and some due to the actual conditions in the eddies (see Gold, 1936). The effect is not significant in well exposed instruments - such as that on Waglan Island which produced the record at lower right in Fig. 5.2(2) - because the wind vane is particularly responsive in hurricane force winds. The natural period of the vane,  $T$ , is given in seconds by the equation:

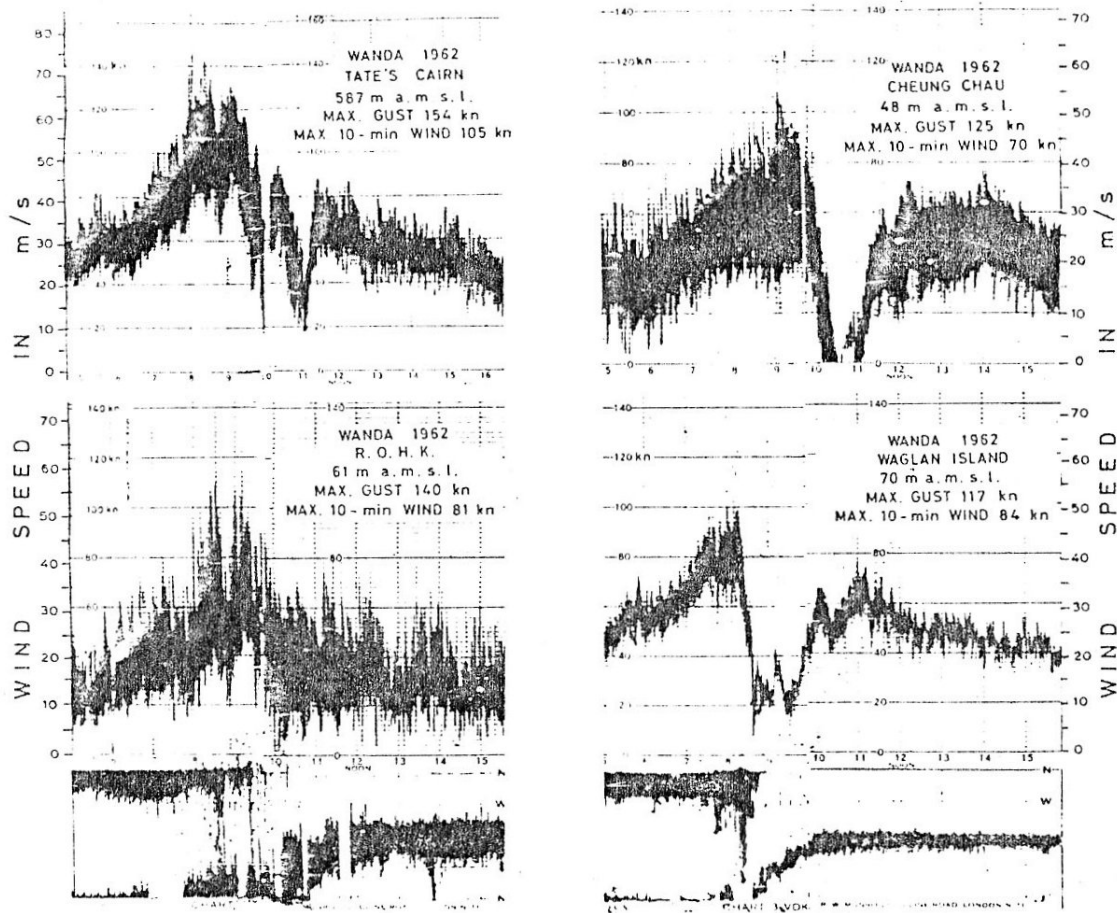


Fig. 5.2 (2). Dines pressure tube anemograms made at stations in Hong Kong during the passage of typhoon Wanda on 1 September 1962. The maximum indicated peak gusts at 140 kn at the Royal Observatory and 154 kn at Tate's Cairn represent true wind speeds of 146 kn (75 m/s) and 165 kn (85 m/s) respectively, after correcting for air density and instrument calibrations.

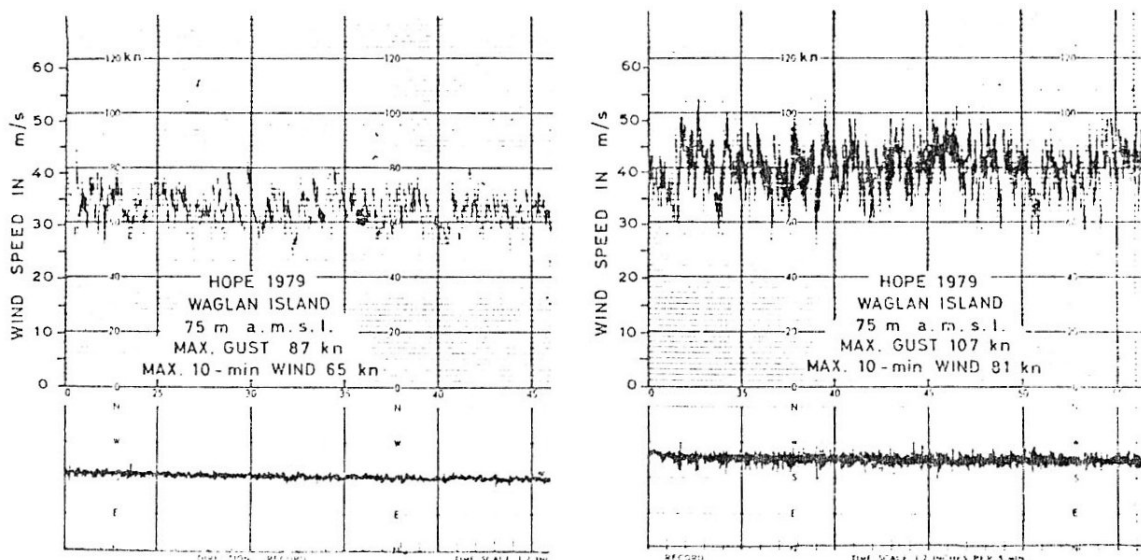


Fig. 5.2 (3) Dines anemometer quick-run records showing 30 minutes of record from Waglan Island during typhoon Hope on 2 August 1979. The heavy vertical lines are at intervals of five minutes and the records run from 0620 to 0645 GMT (left) and from 0530 to 0555 GMT (right). The maximum gust speed of 107 kn on these records corresponds to 111 kn (57 m/s) when corrected. The record from a nearby cup anemometer is at Fig. 5.

$$T = \frac{14.81}{v} \quad 5.2(2)$$

where  $v$  is the wind speed in m/s. When  $v = 60$  m/s the natural period of oscillation is about 2.5s. Figures 5.2(3) and 5.2(4) show the remarkably steady direction of unobstructed typhoon force winds and the effects of topography. Note how the direction trace for the offshore Waglan Island station is almost constant. By comparison the Tates Cairn trace exhibits large amplitude high frequency oscillations caused by horizontal eddies generated by a rough upstream topography.

When the wind speed exceeds about 50 m/s the flow past the mast and pressure pipes sets up a fierce vibration of the instrument which is additional to the shaking of the building in which it is housed. Ink is thrown out of the pen~~/~~reservoirs to spill over the charts and there is a violent and noisy chattering of the direction indicator as successive gusts are recorded. The pens occasionally jump clear of the recording chart as shown in Figures 5.2(2) and 5.2(5). Ball point and felt type pens perform better in this environment. The lifting force on the Dines float in hurricane force winds is also surprisingly large (around 45N at 60 m/s). In the Hong Kong typhoon of September 1937 peak gust speeds exceeded the 61 m/s range of the Dines in use and caused the float to fiercely hammer the top of the cistern. Modified instruments reading to 89 m/s have been subsequently installed.

Three other types of anemometer are occasionally used for high speed conditions. The first is comprised of a small ball, about 25 mm in diameter, held on a supporting rod. The wind force on the ball is sensed by strain gauges or other form of electronic transducer. Such instruments have a natural frequency of about 30Hz and respond very quickly to wind changes. However, they are at a disadvantage in typhoons because large raindrops impacting on the spheres at 50 m/s or more cause over-reading, and indeed often lead to the destruction of the instrument. The second group comprise sonic anemometers which measure the velocity of sound in an

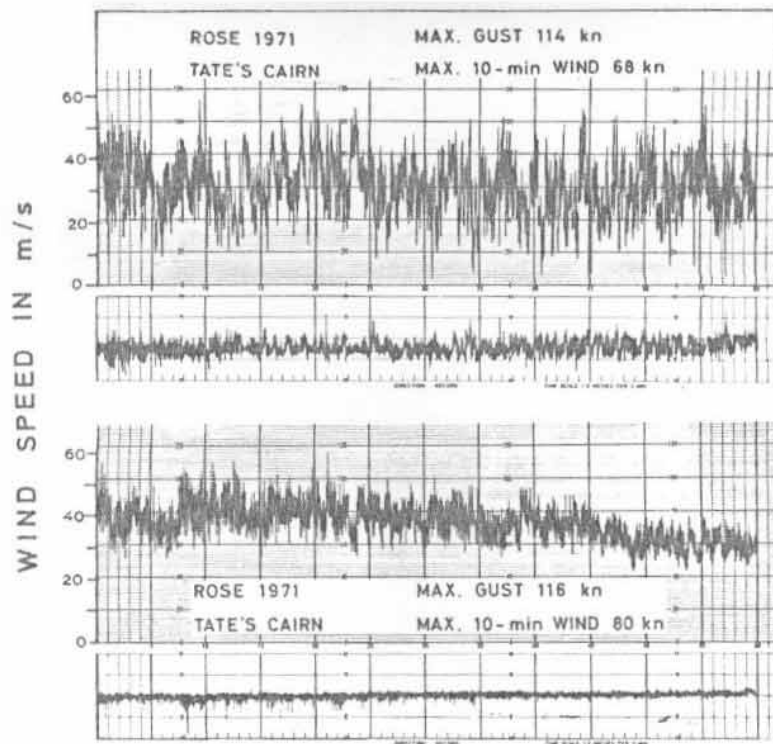


Fig. 5.2(4) Quick-run records from the Dines anemometer 587 m a.m.s.l. at the Hong Kong radar station on Tate's Cairn made during the passage of typhoon Hope on 16-17 August 1971. The times of the upper and lower records were 1800 to 1900 GMT and 1600 to 1700 GMT respectively on 16 August. The maximum gust speed of 116 kn corresponds to a true gust speed of 124 kn (64 m/s) when corrected for density. The highest peak gust speed (not shown) was 66 m/s.

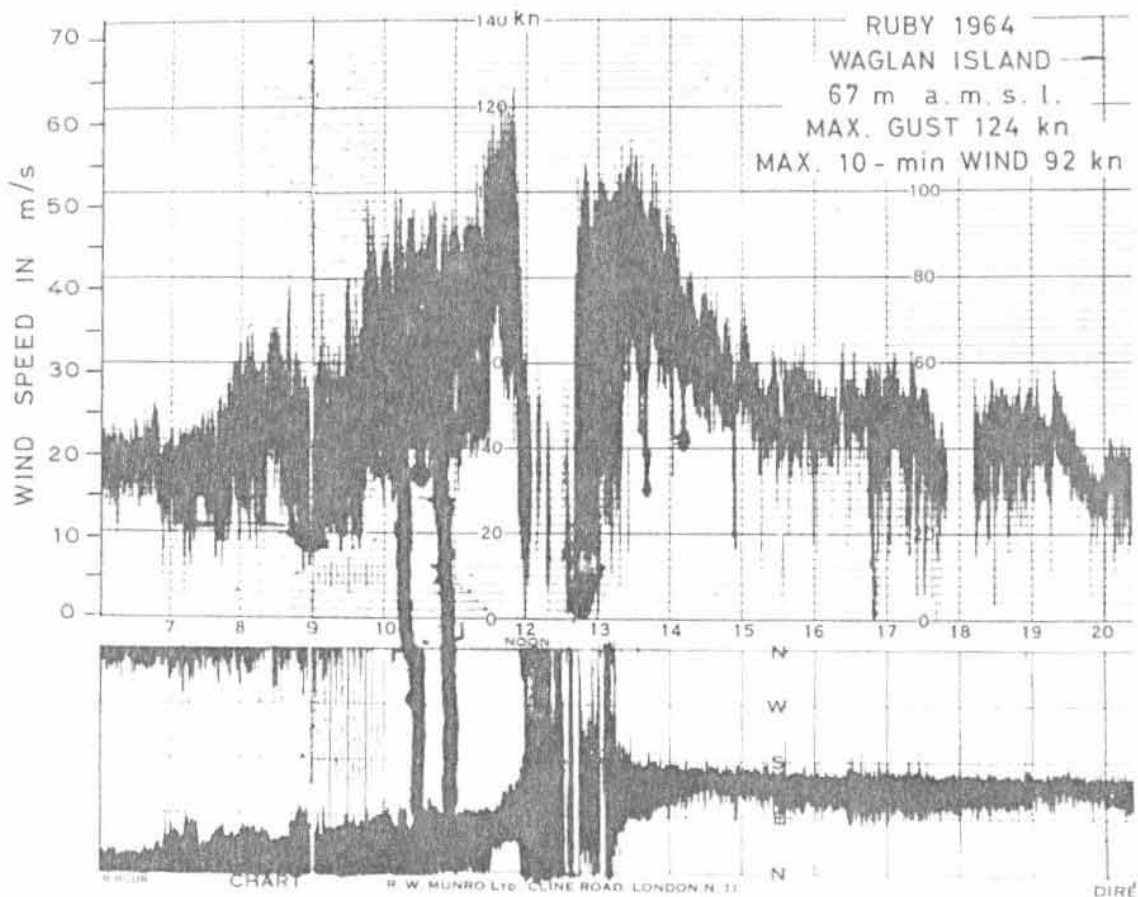


Fig. 5.2(5). The Dines anemometer record from Waglan Island (Hong Kong) during the passage of typhoon Ruby (942 mb) on 5 September 1964. The maximum gust speed of 124 kn becomes 130 kn (67 m/s) when corrected for density. Note the spilling of ink and the missed record when the pen was shaken off the paper by vibrations of the instrument.

airstream along two directions at right angles. From this information the speed and direction of the wind can be derived. They are based on the principle that the speed of sound measured in the direction of a component of the wind velocity will be greater than that in the reverse direction. These instruments are strong, accurate and responsive but their high cost prevents their coming into widespread use. Finally, there is the vortex shedding anemometer as used on the meteorological buoy EB10, ~~to obtain the measurements shown in Fig.14.~~ In this instrument, the Karman vortices shed by a cylinder pass through an ultrasonic beam which is thereby scattered and modulated. Circuits can be arranged to count the vortices and determine the frequency with which they are formed. This frequency can then be converted. Unfortunately, current versions of these anemometers underread by 20% or more in strong winds when accompanied by heavy rain, but further development may overcome this problem.

Measurements of extreme wind speeds in tropical cyclones are frequently lost because of the failure of cup arms, propellers, supporting masts or electricity supplies. In Hong Kong there has been no failure of guyed anemometer masts (Fig. 5.2(6)) but various cup anemometers, including the U.K. Meteorological Office Mk 4, have failed. The Australian Bureau of Meteorology uses a strong pyramidal lattice mast to support Dines anemometers in cyclone-prone areas (Fig. 5.2(6)).

In summary, records from anemometers in high wind conditions can seldom be taken at their face value. They must be assessed in the light of the type of instrument used, its mounting, location and exposure in different directions. Even the intercomparison of two types of anemometer on the same mast is not a simple exercise. For example, efforts have been made to correlate readings made in typhoons by co-located cup and Dines anemometers (Bell, 1961; Mackey, 1971). Attempts have also been made to relate typhoon records from the same type of instrument in the same typhoons but at different locations within about 20 km of one another (Chen 1975, Chin and Leung 1978). These efforts have been only partially successful. Records

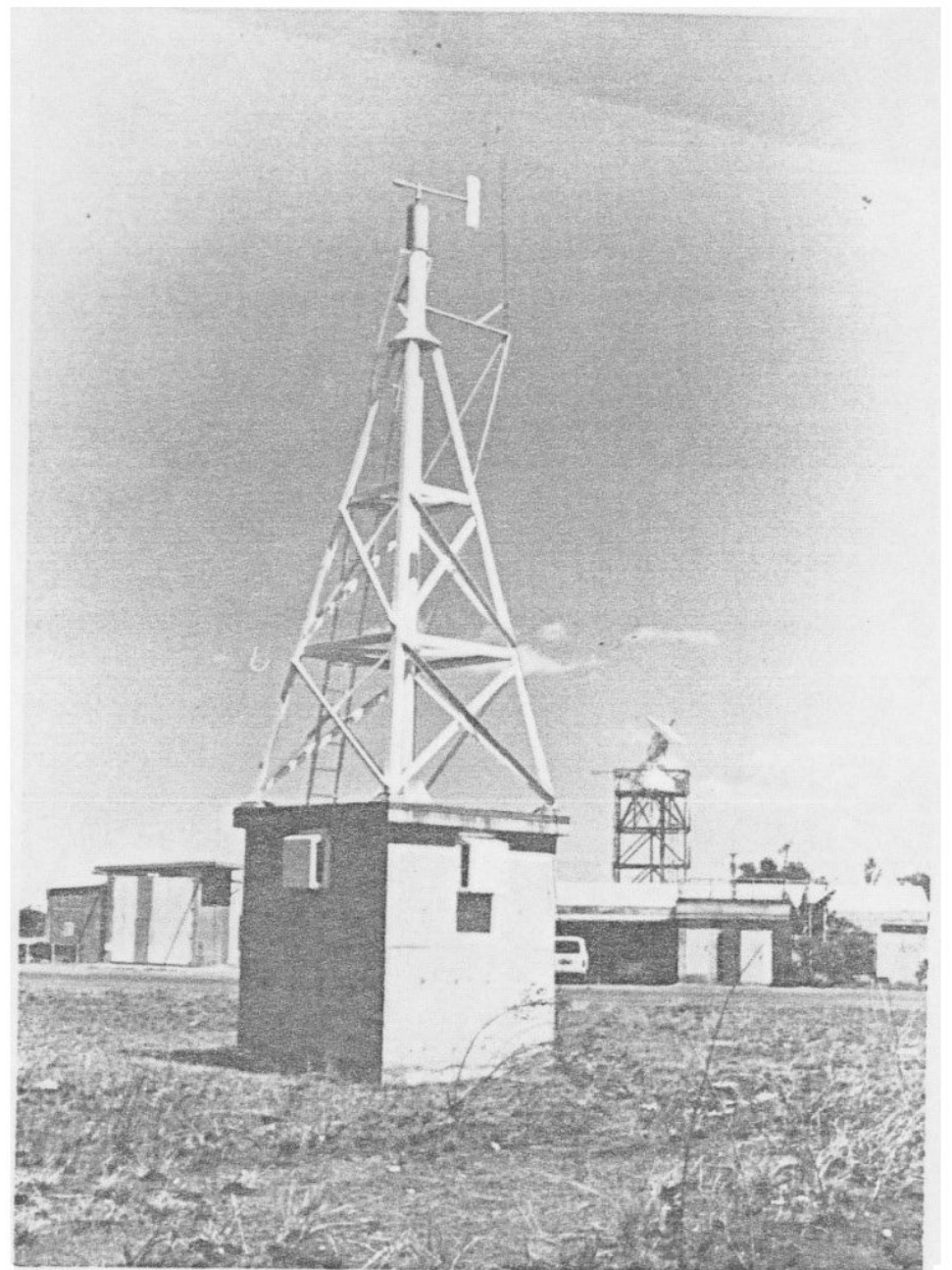
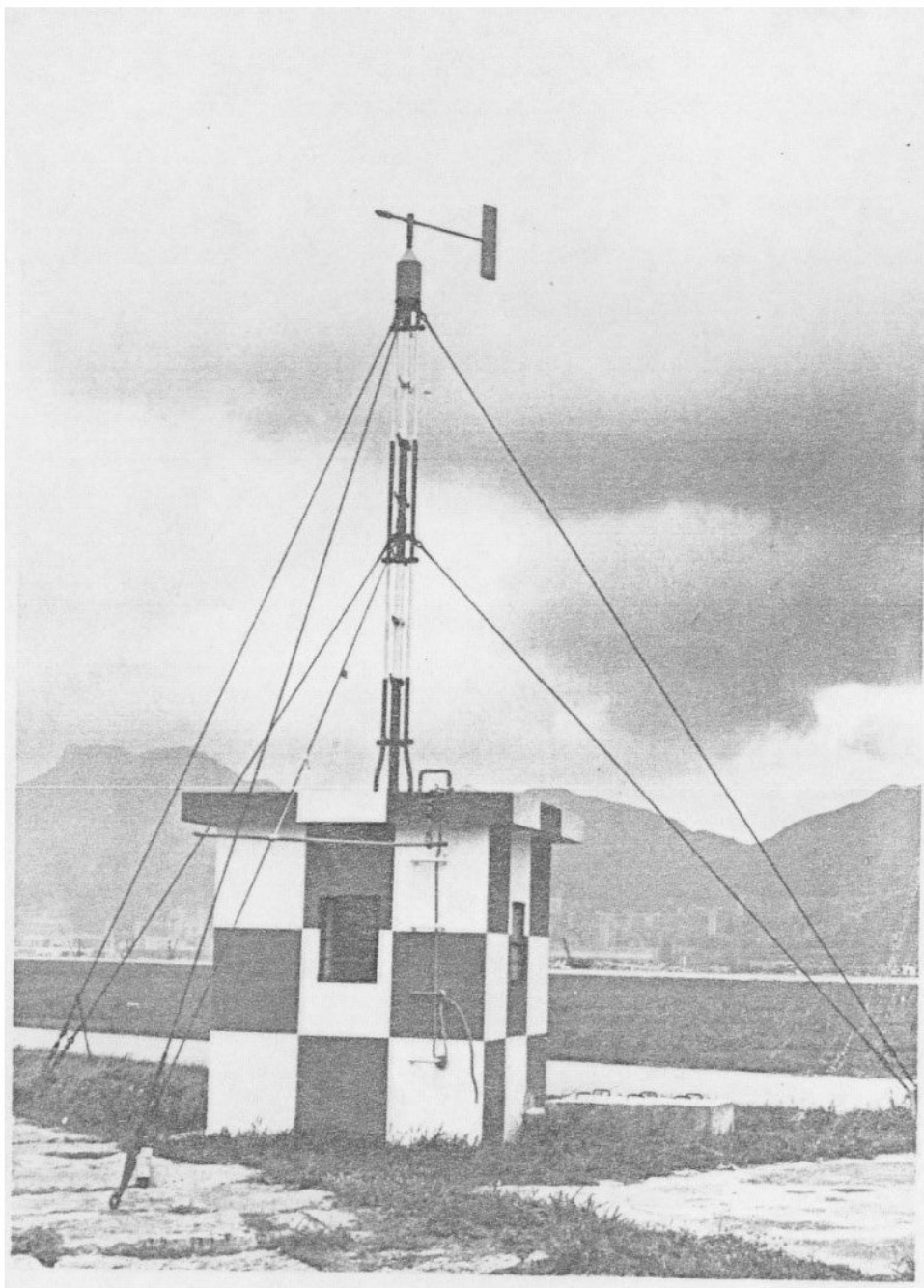


Fig. 5.2.(6) Two methods of securing Dines anemometer masts against tropical cyclone winds. The Royal Observatory Hong Kong stayed mast (left) and the Darwin lattice mast (right).

from anemometers located at places where the surface changes roughness, as in going from sea to land, need particularly careful interpretation. Turbulence generated by surface roughness is discussed in sect. 5.4.2. Pilot of sailplanes and light aircraft are well aware of the remarkable intensity and extent downwind of perturbations in winds caused by hills and lesser obstructions. The point is emphasised by the photograph (Fig 5.<sup>6</sup><sub>λ</sub>(1)) of Karman vortices extending 700 km downwind from the island of Cheju.

### 5.2.2 Beaufort Wind Forces

The intensity of tropical cyclones has always been defined in terms of Beaufort's Scale of Wind Forces (Sect. 1.2), and it is remarkable that for nearly 80 years meteorologists have attempted to assign wind speed equivalents to what sailors have always known to be gales, storms and hurricanes. For this reason a complete discussion of the Beaufort scale and the derivation of wind speed equivalents is ~~discussed~~<sup>presented</sup> in detail.

In the days of sail, ships did not have anemometers on board. (Indeed in 1980 only about 12% of voluntary observing ships have an anemometer~~f~~.) Some method of assessing wind forces was thus required and it was to meet this need that, in 1806, Captain F. Beaufort devised a fourteen degree scale of wind forces (Garbett 1926). In 1807 Beaufort reduced the number of forces in his scale from fourteen to thirteen - by combining two of the lower forces - and defined each one in terms of the canvas that a man-of-war could show to the wind and the speed with which she might travel (Table 5.2(1)). In 1838 the Lords Commissioners of the Admiralty issued a Memorandum(containing two significant misprints!) to adopt Beaufort's scale of wind forces for use in the Royal Navy. Its use then spread to the British Mercantile Marine and, later, to ships of other countries. The introduction of double topsails in about 1850 led the 1872 Maritime Congress

Table 5.2(1)

Beaufort Scale of Wind Force 1807

<u>Force</u>	<u>Name of Wind</u>	<u>Description of its effect on a Frigate</u>	
0	Calm		
1	Light Air	just sufficient to give steerage way	
2	Light Breeze	with which a well- conditioned man-of- war, under all sail and clean full, would go in smooth water, from -	1 to 2 knots
3	Gentle Breeze		3 to 4 knots
4	Moderate Breeze		5 to 6 knots
5	Fresh Breeze		Royals &c.
6	Strong Breeze	in which the same ship could just carry close hauled -	Single-reefs and top- gallant sails
7	Moderate Gale		Double-reefs, jib, &c.
8	Fresh Gale		Triple-reefs, courses, &c.
9	Strong Gale		Close-reefs, and courses.
10	Whole Gale	with which she could only bear -	Close-reefed main topsail and reefed foresail.
11	Storm	with which she would be reduced to -	Storm stay- sails.
12	Hurricane	to which she could show	No canvas.

to suggest modifications to the scale and these were approved for international use in weather reports at the International Meteorological Committee (I.M.C.) meeting in Utrecht in 1874.

With the passing of sail the practice arose of judging the wind force from the state of the sea surface. In 1939 the I.M.C. agreed, at its meeting in Berlin, to adopt, provisionally, Capt. Peterson's criteria for estimating Beaufort's wind forces from the appearance of the sea surface. The wind equivalents for Beaufort's wind forces as determined using Peterson's criteria were derived in 1906 by Sir George Simpson (Table 5.2(2)). He had compared a large number of wind force observations made by experienced observers at five stations in the British Isles with the records from nearby well exposed anemometers 10 m above the sea or ground (Simpson 1906). Two of these stations were inland and three were coastal. The observation of the force of wind at the hour compared with the "run" of the wind from 30 minutes before to 30 minutes after the hour as recorded by the anemometers. The final figures agreed closely with the following relationship between the mean hourly wind speed  $v$  in meters per second and the Beaufort Force  $B$ :-

$$v = 0.836B^{3/2} \quad 5.2(3)$$

There was also in existence a series of equivalents known as the Seewarte Series (Table 5.2(2)) which were derived from four independent sets of observations, two from ships in the open sea, one from German light-vessels and two from coastal stations in Norway and England (Köppen 1898) and they agreed well with the relationships:-

$$v = 1.35 B^{7/6} \quad 5.2(4)$$

It was obviously undesirable to have two different sets of speed equivalents and so, at its London meeting in 1921, the I.M.C. asked Simpson to derive a definite set of equivalents between Beaufort forces and wind speed. Simpson (1926) then proposed a compromise set of equivalents in which he averaged, in a rather special way, the two series

(2)

Table 5.2. Equivalent speeds in metres per second

Beaufort No.	0	1	2	3	4	5	6	7	8	9	10	11	12*
Seewarte series	0	1.7	3.1	4.8	6.7	8.8	10.7	12.9	15.4	18.0	21.0	24.4	-
Simpson 1906 series	0.1	0.8	2.4	4.3	6.7	9.4	12.3	15.5	18.9	22.6	26.4	30.5	32.7
Proposed CMM-IV	0.2	2.0	3.6	5.6	7.8	10.2	12.6	15.1	17.8	20.8	24.2	28.0	30.1

\* All speeds above or equal to the given inferior limit

of observations referred to above. The new equivalents were adopted by the I.M.C. at its meeting in Vienna, in 1926, but they did not prove satisfactory and at the meeting in Paris in 1946 they were replaced by Simpson's original 1906 equivalents. These mean hourly wind speed equivalents are still in use today.

It should be noted that it is Captain Peterson's sea state equivalents which are difficult to convert to actual speeds, not Admiral Beaufort's original scale. The Beaufort scale is a scale of wind effects, not speeds, but the effects on a frigate can be readily related to wind speed. By comparison, the wind effect on the sea state depends on a number of variables such as air temperature and density, atmospheric stability, sea currents, swells, and fetch, duration, and characteristics of the wind. It is this dependence of sea state on factors other than wind speed which has led to the difficulty in determining equivalents.

Frost (1966) compared observations of Beaufort forces and wind speed measurements made on British Ocean Weather Ships between 1960 and 1964. These show that in the open sea the speed equivalents are:-

$$v = 1.38 \left( \frac{z}{10} \right)^{1/5} B^{7/6} \quad 5.2(5)$$

where z is the height of the anemometer in metres. If the winds are measured at a height of 10 m this reduces to practically the same relationship as was found for the Seewarte series given in equation (5.2(4)).

Frost also found that the effect of the stability of the atmosphere on the wind speed equivalents at 10 m height was so small that it could be neglected for practical purposes. However, he showed that in coastal waters the equivalents depended markedly on the fetch of the wind such that

$$y v_{10} = 0.61 B^{14/9} \quad 5.2(6)$$

where y is non dimensional quantity which is a function of the fetch

and varies from a value of 0.76 for a fetch of 40 km to a value of about 0.94 for fetches in excess of 150 km. For a fetch of 35 km,  $y = 0.73$  so that

$$v_{10} = 0.84 B^{14/9} = 0.84B^{1.56} \quad 5.2(7)$$

which is similar to the relationship found by Simpson in 1906 and adopted by the W.M.O. Frost therefore suggested that the wind speed cannot be estimated from the appearance of the sea surface in coastal waters unless allowance is made for the fetch of the wind. Beaufort forces, as estimated from the sea surface, are only valid over the open sea remote from land when the wind has been blowing long enough for a steady state to be obtained.

The current (1980) W.M.O. equivalents (i.e. Simpson 1906), the Seewarte Series and new equivalents proposed by the fourth session of the W.M.O. Commission for Maritime Meteorology (C.M.M. IV) are given in Table 5.2(2). The wind speed equivalents proposed by CMM IV have not yet (1980) found general acceptance because, inter alia, the inferior limit of Force 12 is 2.6 m/s less than the current scale. This would imply a new definition of hurricane or typhoon in terms of wind speed.

### 5.2.3. Average windspeeds and gusts

The surface wind at a location is never steady but continuously fluctuates as atmospheric eddies pass by. The frequency of the velocity fluctuations depend upon the size of the eddies and the speed with which they are carried along by the mean wind. In tropical cyclones, eddies occur in a wide spectrum of sizes. The wind fluctuates over intervals of less than a second to intervals of a few seconds - as shown in Figs. 5.2(3) and 5.2(4) - and on up to periods of ten or more hours as illustrated in Fig. 5.2(2). Most anemometers do not resolve the faster variations. The relatively long response time of these instruments results in short-period fluctuations being smoothed out. Indeed, it is usual to average over some period when determining a wind speed, either instrumentally or subjectively.

Wind speeds are commonly averaged over one year, one month, one day, one hour, ten minutes, one minute, three seconds, or one second. Peak gust speeds and the "fastest mile" of wind are also used for various purposes. A wind averaged over a long period will contain some shorter periods which have higher (or lower) speeds. It is clear, therefore, that a wind speed should not be given without indicating over what period it has been averaged.

Published records mostly consist of hourly or ten minute means and the highest peak gust. However, average speeds over intermediate periods are often required. Durst (1960) found that, in the case of quick-run records from a Dines anemometer sited over open grassland at Cardington in England, the frequencies of 5s and other short-period averages tended to have a Gaussian distribution about the parent 10 min mean. He further showed that the ratio of the standard deviation - of the short-period means about the parent long-period average - to the long-period mean tended to be constant for different values of the latter.

Using these two facts he was able to derive, from statistical considerations, the probable maximum short-period mean corresponding to a given one hour mean. There will be, for example, 60 times more one-second averages in a given hour of record than one-minute averages. The larger sample has the same (parent) mean but will tend to contain larger extremes as given by the normal distribution. It is usual to express the probable maximum short-period average in terms of a "gust factor" to apply to the long-period mean.

In 1961 it was first shown that extreme winds in typhoons displayed characteristics similar to the lesser winds at Cardington and that they could be analysed in the same way (Bell 1961). Since that time many other quick-run records in typhoons have been obtained at Hong Kong stations and records have been obtained from an oil rig in hurricane Camille (1969) and a buoy in hurricane Betsy (1965). Some results from analyses of these observations are given in Table 5.2(3) and plotted in Fig. 5.2(7), which illustrates three well known phenomena. Firstly, gust factors are greater over urban areas (Mary) than over open grassland (Cardington). Secondly, gust factors are less over the ocean (Betsy and Alice) than over open grassland (Cardington) and, thirdly, gust factors decrease with height (Rose and Hope).

the heavy curve fitted to the observations made in hurricane Betsy and typhoon Alice best approximates conditions over the sea near standard anemometer height in tropical cyclones. Table 5.2(4) gives the gust factors indicated by the Alice/Betsy curve for different parent and short-period averages. These factors can be used to find, for example, the probable maximum 1-min mean or the peak gust corresponding to a given 10-min mean. It should be noted that peak gusts are not true averages but depend on gust magnitude and duration and on the response characteristics of the anemometer. The extreme gusts in tropical-cyclone wind records usually correspond to about a 2s average for the normal Dines and a 1s average for propellor or cup anemometers.

Table 5.2(3) Details of the anemometer records used to calculate the gust factors given in the lower part of the table

Tropical cyclone	Height above mean sea-level m	Date	Station	Peak gust m/s	Peak wave height m
T. Alice (E'ly)	54.9	19 May 1961	Waglan	37.3	-
T. Rose (E'ly)	74.6	17 Aug 1971	Waglan	55.1	15.2*
T. Hope (W'ly)	74.6	2 Aug 1979	Waglan	57.8	-
T. Hope (SW'ly)	61.0	2 Aug 1979	Cape D'aguliar	66.9	-
H. Betsy (SE'ly)	13.0	7 Sep 1965	Buoy	42.9	15.2
H. Camille (TW)	30.5	17 Aug 1969	T.W. Oil Rig	76.9	23.60
H. Camille (62A)	27.1	17 Aug 1969	S. Pass 62A Rig	52.8	21.95
T. Mary Cardington (not in a T.C.)	60.9 15.2	9 Jun 1960 6 Jan 1928	R.O.H.K. Cardington	55.6 32.6	-- --

Factors to apply to an hourly mean wind speed to obtain the probable maximum average speed over the indicated periods

Anemometer type	600s	300s	60s	30s	10s	5s	3s	Observed peak gust factor
Dines	1.08	1.11	1.18	1.21	1.30	1.35	1.42	1.51
Dines	1.03	1.04	1.10	1.15	1.21	1.24	1.30	1.35
Dines	1.05	1.08	1.13	1.14	1.22	1.27	1.33	1.39
Cup.MK.IV	1.09	1.11	1.15	-	-	-	-	1.31
Prop	1.07*	1.10*	1.16	-	1.28	-	1.38*	1.60
Prop	1.05*	1.10	-	-	-	-	1.40*	1.48
Prop	-	-	1.16*	1.21	1.29	1.33	1.47	1.62
Dines	1.05	1.09	1.28	1.42	1.64	1.72	-	2.20
Dines	1.08	1.13	1.24	1.32	1.42	1.48	1.56*	1.77

\* estimated

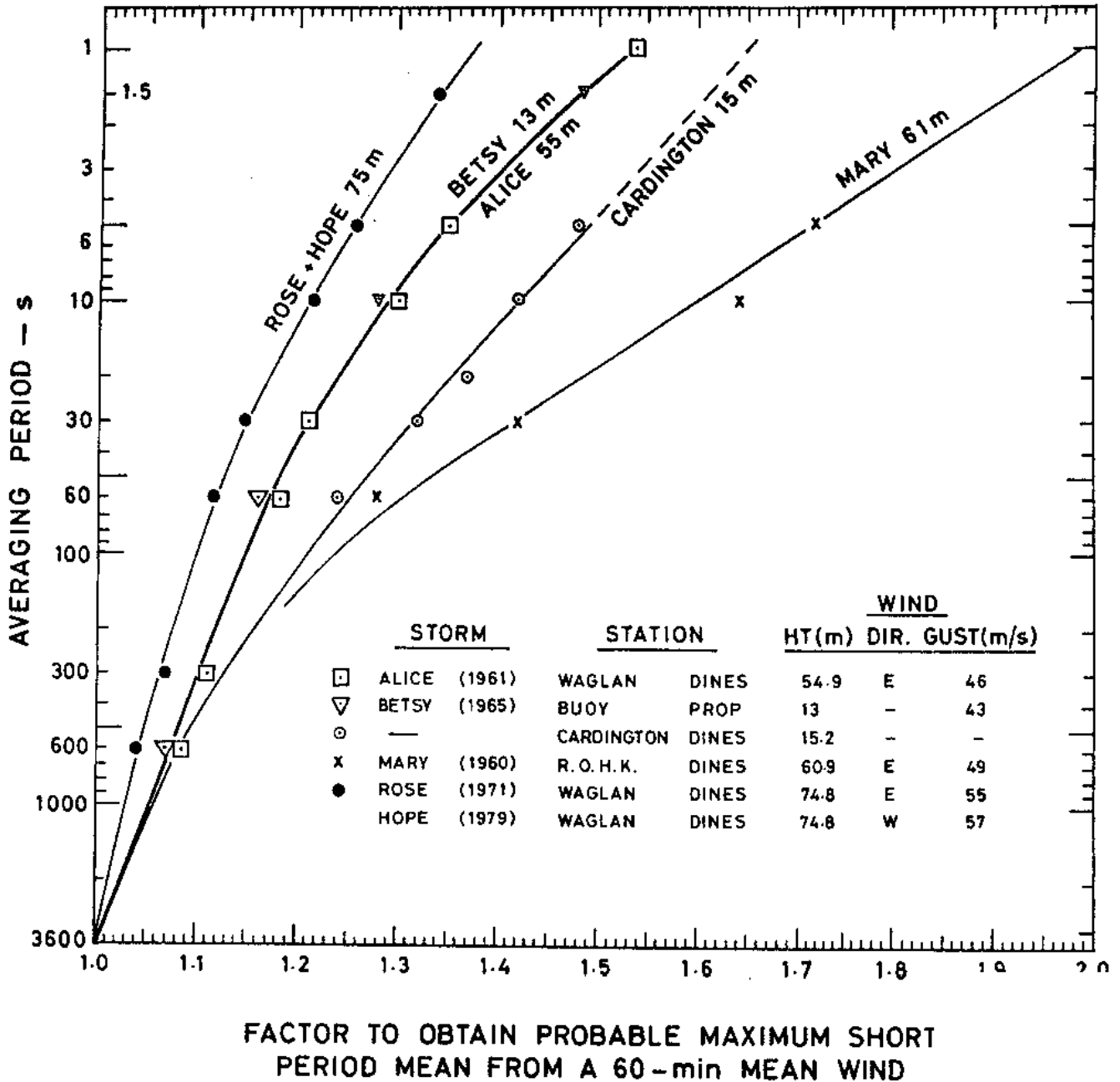


Fig. 5.2 *h* (7). Factors to apply to a mean-hourly wind speed to obtain probable values of the maximum wind speed, averaged over shorter periods of time. The curves labelled Cardington and Mary are for land stations.

Table 5.2(4) Factors to apply to an hourly-mean wind over the sea near the 10 m level to obtain the probable maximum short-period means. Other factors within this set are also given.

1h	600s	300s	60s	30s	10s	5s	3s	Gust (~1s)
1	1.07	1.10	1.17	1.21	1.29	1.35	1.40	1.54
	1	1.03	1.09	1.13	1.21	1.26	1.31	1.44
		1	1.06	1.10	1.17	1.22	1.27	1.40
			1	1.04	1.10	1.15	1.20	1.32
				1	1.06	1.11	1.15	1.27
					1	1.05	1.08	1.20
						1	1.03	1.14
							1	1.11

Table 5.2(5) indicates how the gust factors at the Royal Observatory during typhoon gales have increased over the period 1950-1979 as the surrounding area has been developed. This increase is in spite of the anemometer head having been raised during the period (Bell 1961) in an attempt to reach less turbulent conditions.

### 5.3 Low-Level Wind Field

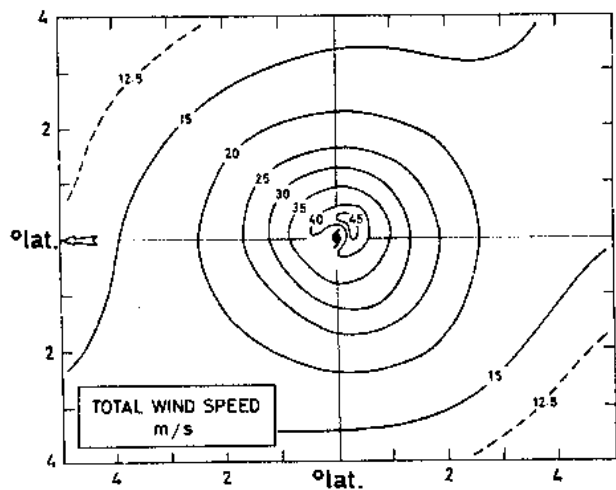
A complete description of surface winds in a typhoon over the open ocean is rarely available. Ship reports are common in the outer fringes but ships make every effort to avoid the violent inner regions. Of those which approach the centre, few have anemometers and their position estimates are often unreliable. A notable exception was obtained in 1935 when officers of the Imperial Japanese fourth Fleet were able to define the wind field in a typhoon of central pressure 960mb and maximum wind speed 42m/s. The introduction of automatic weather stations on coral cays and other low lying islands has provided improved information in recent years, but, even so, some form of short term compositing is required to fill in the details. By comparison to this lack of surface observations, however, aircraft reconnaissance flights between 300m and 1 Km have provided excellent descriptions of the low level wind fields in many Atlantic hurricanes and northwest Pacific typhoons. These data will therefore be used in the bulk of the following discussion. The variation of winds with height in the friction layer is described in Section 5.4

#### 5.3.1 Radial Variation of Wind Speed

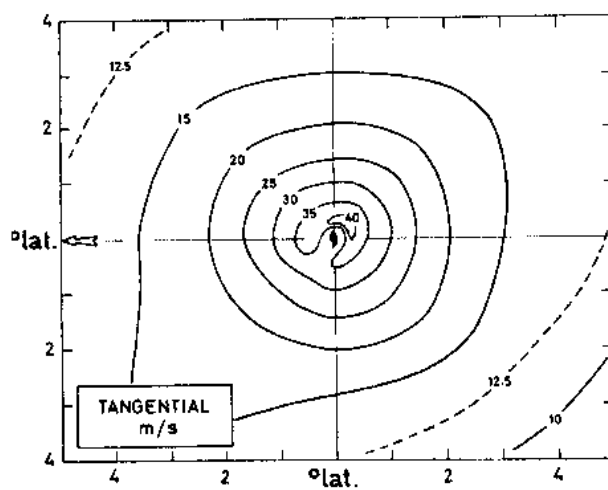
The low level wind structure in a typical typhoon consists of an eye region containing weak, and at times calm, winds, a rapid increase near the radius of maximum winds and a gradual decrease at larger radius. But this simple description glosses over a large variability. As can be seen in Figure 5.3.1(1) the profile shape, the maximum wind speed and the radius of maximum winds vary considerably from cyclone to cyclone and even within the

Table 5.2(5) The ratio of the Dines peak gust speed to the hourly mean wind speed (gust factor - G.F.) in strong winds ( $\geq 11$  m/s) and in tropical cyclone gales ( $\geq 17$  m/s) at the Royal Observatory, Hong Kong

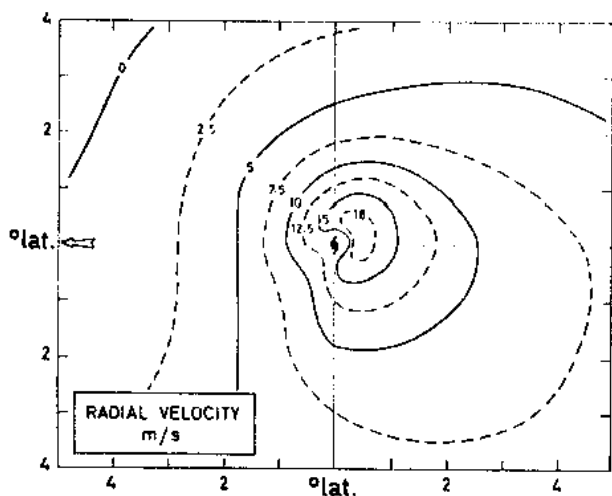
Year	Annual average G.F.		Decade average G.F.	
	Strong	T.C. gale	Strong	T.C. gale
1950	1.52	1.74	1.69	1.75
1951	1.51	1.71		
1952	1.59	-		
1953	1.69	1.79		
1954	1.66	1.82		
1955	1.74	-		
1956	1.61	-		
1957	1.75	1.71		
1958	1.85	-		
1959	2.01	-		
1960	2.05	2.06	2.23	2.09
1961	1.99	1.95		
1962	2.07	2.06		
1963	2.28	-		
1964	2.18	2.15		
1965	2.26	-		
1966	2.51	2.34		
1967	2.25	-		
1968	2.45	1.95		
1969	2.27	-		
1970	2.32	-	2.39	2.29
1971	2.43	2.20		
1972	2.39	-		
1973	2.38	2.26		
1974	2.62	-		
1975	2.57	-		
1976	2.26	-		
1977	2.30	-		
1978	2.16	-		
1979	2.46	2.41		



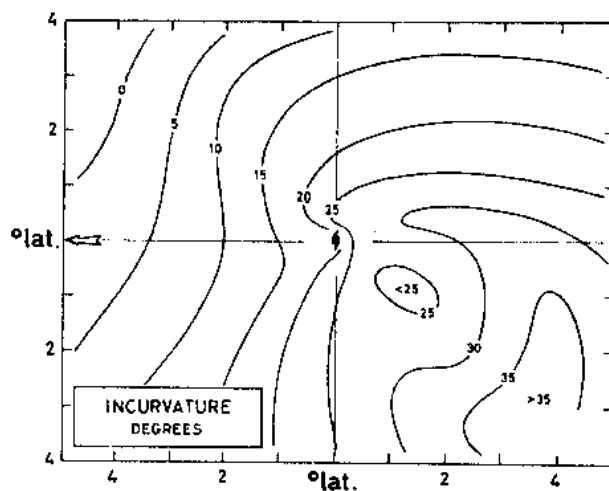
(a)



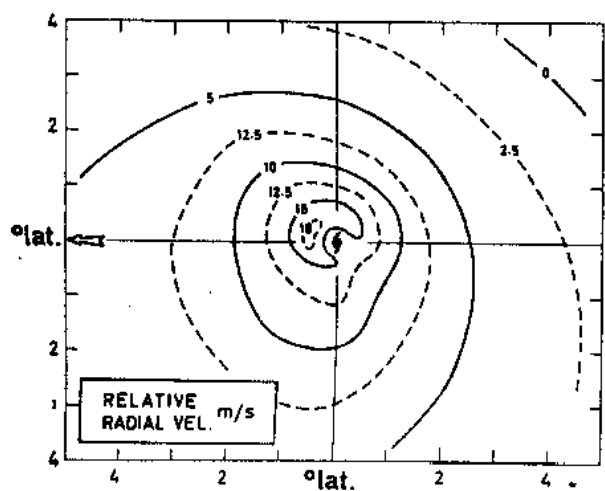
(b)



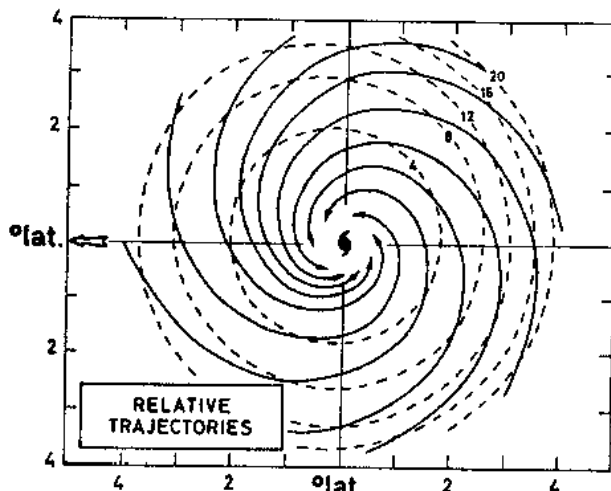
(c)



(d)



(e)



(f)

Fig.5.3.1.(1) The average low-level (about 300 m) wind field from 13 large typhoons with circulations greater than 750 km in radius. The relative radial velocity (e) and trajectories (f) are drawn relative to the moving centre. The arrow indicates the direction of storm movement in all figures and the dashed lines in (f) indicate travel time in hours along a trajectory to a point  $0.5^\circ$  lat from storm centre. (Redrawn from Hughes 1952)

life cyclone of a single cyclone. The situation is further complicated by tropical cyclones which may have similar core region characteristics but very different outer circulations; a small cyclone such as Hurricane Tracy (e.g. Holland, 1980) may extend gale force winds over less than 50 Km radius, while a large system such as Typhoon Tip (Dunnavan and Diercks, 1980) may extend to more than 1000 Km. Indeed, Tracy could have been accommodated inside the eye of some larger systems! Such variability is not insignificant as it has a considerable impact on the extent and magnitude of the damage which can result.

In an attempt to rationalise these structural differences, Merrill (1983) suggested a breakdown into three quasi-independent categories: intensity, strength and size. These are illustrated in Figure 5.3.1(2) as changes from an initial profile. Intensity describes the magnitude of the maximum wind speed (or central pressure if no wind speed observations are available). Pure intensity change then typically occurs as an inward contraction of the radius of maximum winds and can generally be achieved by a slight rearrangement of angular momentum within the cyclone. Strength describes the average wind speed within 300 Km of the cyclone centre and thus, in essence, the horizontal extent of hurricane force winds. Strength changes are constrained by the availability of sufficient angular momentum in the typhoons outer circulation. As discussed in Section 4.3 the size of a typhoon is defined by the extent of gale force winds or, equivalently, the mean radius of the outer most closed isobar.

Thus an intense, but small and weak typhoon will only affect areas directly in its path; a strong typhoon may cause significant damage two or three hundred kilometers to either side of its track; and a large system will be noticeable over many hundreds of kilometers.

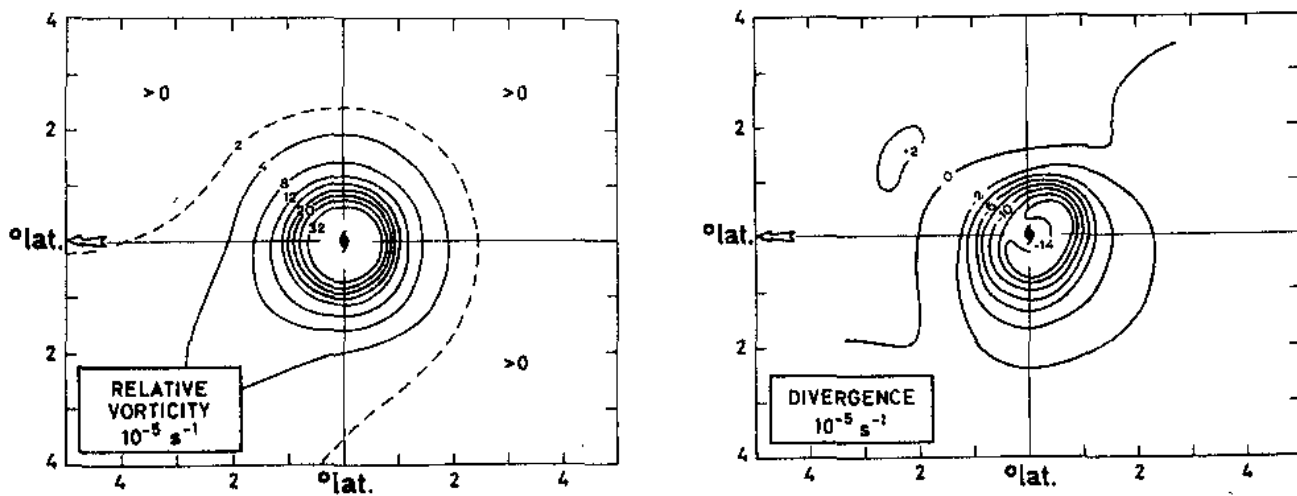


Fig. 5.3.1.(2) The divergence and relative-vorticity fields in the mean tropical cyclone moving in the direction of the arrow. The divergence field can also be read in terms of vertical motion (cm/s) with negative values indicating upward motion. (Redrawn from Hughes 1952)

A number of analytical approximations to these winds profiles have been developed and used in a variety of applications ranging from theoretical research to storm surge modelling and operational forecasting. Of these the most successful seem to be the modified Rankine vortex and the analytic model of Holland (1980).

An examination of the wind profiles in Figure 5.3.1(1) will indicate that to a first approximation they may be described by a solid body rotation inside the radius of maximum winds and an exponential decrease outside. This basic shape lead Depperman (1947) to suggest that these radial profiles could be approximated by a Rankine vortex:

$$v/r = C_1 \quad r \leq R \quad 5.3.1 (1)$$

$$vr = C_2 \quad r \geq R \quad 5.3.1 (2)$$

Where R is the radius of maximum winds and  $C_1, C_2$  are appropriate constants.

Equations 5.3.1(1,2) describe a vortex which is in solid body rotation inside the ~~the~~ maximum wind belt and has a constant relative angular momentum outside this region. This constant angular momentum curve is physically consistent for a system with no frictional losses so that the inflowing air simply conserves relative angular momentum. However, tropical cyclones lose a substantial amount of angular momentum to surface and other frictional losses, and Hughes (1952) proposed a modified Rankine vortex in which Equation 5.3.1(2) becomes

$$vr^x = C_3 \quad 5.3.1(3)$$

Where  $x$  is some constant less than unity. Empirical determinations by Hughes (1952), Riehl (1954, 1963) and Gray and Shea (1973) have indicated that  $x$  typically has between 0.4 and 0.6, though values ranging from nearly zero to 0.8 have been observed.

This modified Rankine vortex, with empirically determined constants  $C_1$ ,  $C_3$  and  $x$ , will provide a good approximation to the wind field within 100 Km of the maximum wind belt. It is also simple and amenable to analytic studies. However, it tends to overestimate the outer region wind fields and requires a precise knowledge of the radius and speed of maximum winds. A derivation of the empirical constants is also subject to inaccuracies in wind estimates within the typhoon circulation. These considerations lead Holland (1980) to suggest an alternative profile based on pressure observations.

Holland's technique is based on the observation by Scholomoer (1954) that, after normalising to remove variations due to differing ambient to central pressure differences, tropical cyclone pressure profiles closely resembled a family of rectangular hyperbolae. They may therefore be approximated by:

$$p = p_c + (p_n - p_c) \exp(-A/R^B) \quad 5.3.1(4)$$

Where  $p$  is the pressure at radius  $r$ ,  $p_c$  is the central pressure,  $p_n$  the ambient pressure (usually the outermost closed isobar); and  $A$  and  $B$  are scaling constants. Using the gradient wind relation the corresponding wind profile is then:

$$V_g = \left\{ AB(p_n - p_c) \exp(-A/R^B) / \left[ \int r^B + \frac{r^2 f^2}{4} \right]^{\frac{1}{2}} - \frac{r f}{2} \right\} \quad 5.3.1(5)$$

Where  $V_g$  is the gradient wind at radius  $r$ ,  $\rho$  the air density, (which is to a good approximation constant) and  $f$  the Coriolis parameter. In the vicinity of the maximum winds the Coriolis effects are small and the wind field may be approximated by the cyclostrophic wind:

$$v_c = \left[ AB(p_n - p_c) \exp(-A/r^B) / \rho r^B \right]^{1/2} \quad 5.3.1(6)$$

Then, by setting  $\frac{dv_c}{dr} = 0$  the radius of maximum winds will be given by

$$R = A^{1/B} \quad 5.3.1(7)$$

Using Equations 5.3.1(6,7), the maximum winds will then be:

$$v_m = \left( \frac{B}{\rho e} \right)^{1/2} (p_n - p_c)^{1/2} \quad 5.3.1(8)$$

Thus, given a few pressure observations in the typhoon circulation and a central pressure estimate to empirically determine the scaling constants  $A$  and  $B$ , the gradient wind profile, radius of maximum winds and maximum wind speed may be quantitatively estimated. If  $R$  and  $v_m$  are also known, a quite accurate profile can be determined by iterative processes. This technique is easily programmed into a hand held calculator and is in use at a number of forecasting centres. It does, however, tend to smooth out the maximum pressure gradients and thus underestimate the maximum wind speeds slightly. Further, total wind differences from the gradient tangential component will not be included.

### 5.3.2 The 300 m wind field

In a classic paper, Hughes (1952) composited 500 wind reports obtained from 40 low-level - about 300 m - reconnaissance flights by U.S. Navy aircraft into 13 Pacific tropical cyclones during the period 1945-47. Winds were obtained from the measurement of aircraft drift at intervals of about 15 minutes. The sample chosen for analysis consisted of large storms with circulations greater than 750 km in radius. The mean of a sample of a smaller storm was similar in all respects except size.

This early work remains a classic because of the low level at which the flights were made. Although the subsequent introduction of Doppler and inertial navigation systems greatly improved the frequency and accuracy with which measurements of wind could be made, most flights carrying these instruments have been made at the 700 mb level ( $\sim 3$  km).

The distribution of wind velocity found by Hughes is shown in Fig. 5.3.2 (1)a.

Note how the winds are stronger to the right of the direction of motion than to the left. A large part of this asymmetry is due to the storm's motion: to the right, the motion and the cyclonically rotating winds are complementary; to the left they are opposed. In the Southern Hemisphere cyclones rotate clockwise and the strongest winds are to the left of the motion. However, there is usually more asymmetry than due to the motion alone, and on occasions the maximum winds may be found to the left of the motion, or front, or back. The underlying mechanisms responsible for these additional, or anomalous, asymmetries are not well understood, though Shapiro (1983) has shown that differential interactions with the underlying surface may cause some variations. In essence Shapiro showed that frictionally induced convergence and maximum winds may be aligned in different quadrants, depending on the storm's speed of motion. Slow moving storms have a maximum in the rear, but as the translational speed increases the maximum will shift to the right and even into the front right quadrant.

Izawa (1964), Shea and Gray (1973), Frank (1977) and Holland (1983) all obtained similar patterns for wind fields at 800 m to 1 K m height using both aircraft reconnaissance and rawinsonde compositing techniques. It is also notable that the large typhoon fields in Figure 5.3.2(1) differ from the small typhoon fields (not shown) only in the extent of gale and strong winds; conditions in the inner core region remain quite

similar. This is supported by Merrill (1982) who showed that there is a very poor correlation between typhoon size and intensity.

There is little difference between the total wind field in Fig. 5.3.2 (1)a and the tangential wind field in Fig. 5.3.2(1)b because the tangential wind speeds are much greater than the radial components, which are shown in Fig. 5.3.2 (1)c. The radial component is much greater in the rear than in the front quadrants so that it is in the rear that the angle of incurvature is greatest (Fig. 5.3.2(1)d). When the motion of the storm (average 5m/s) is removed from the velocity field the radial inflow relative to the moving centre is seen to be greatest in the front quadrants (Fig. 5.3.2 (1)e). In consequence it is the air in the right front quadrant which approaches the centre most rapidly, a point made explicit in Fig. 5.3.2(1)f where the relative trajectories are shown. This feature explains how cold air to the poleward of a westward moving typhoon can quickly find its way to the centre and weaken the storm. Conversely, typhoons which have recurved can persist with cold air to the north for some days as the front-right quadrant continues to feed warm air (rotate Fig. 5.3.2(1)f) to the centre and the penetration of cold air is delayed or prevented (sect 13).

The relative vorticity and divergence fields associated with the mean tropical cyclone are shown in Fig. 5.3.2(2), where

$$\text{Divergence} = \frac{1}{r} \left( -\frac{\partial r V_r}{\partial r} + \frac{\partial V_\theta}{\partial \theta} \right) \quad 5.3.2(1)$$

$$\text{Vorticity} = \frac{1}{r} \left( \frac{\partial r V_\theta}{\partial r} + \frac{\partial V_r}{\partial \theta} \right) \quad 5.3.2(2)$$

Since the density is practically constant over the area shown the pattern of divergence can also be considered as representing that of horizontal mass divergence. This pattern can then be read as the vertical motion at 1 km, although neglect of density changes could lead to an overestimate of ascent speed of up to 10%. Convergence is strongest in the left rear of the storm. The subsidence area ahead and to the left of the typhoon - usually accompanied by fine weather - is well marked and remarkably large. Gray and Shea (1973) find intense convergence just outside the radius of maximum winds amounting to  $23 \times 10^{-5}$  per sec. at 900 mb. This is equivalent to the mass of the atmosphere in a volume in this region being totally evicted upwards in one hour.

The relative vorticity (Fig. 5.3.2 (2)) and the absolute vorticity are everywhere cyclonic. The relative vorticity is largely the sum of the shear and curvature terms (or the  $\frac{1}{r} \frac{\partial r v_\theta}{\partial r}$  term in ~~Eq.~~ <sup>Eq.</sup> 5.3.2(2)), the former is anticyclonic and ranges from one half to four times the Coriolis parameter at the mean latitude of the storms. However, the curvature term is cyclonic and the high wind speeds and small radii of curvature combine to make this term everywhere greater, in absolute value, than the shear term. Near the centre the shear term has its largest anticyclonic value and the relative vorticity has its largest cyclonic value.

### 5.3.3      The Surface Wind Fields

As mentioned in the introduction to this low-level wind field discussion, the first good description of the surface wind field in a typhoon was provided by observations from the Imperial Japanese Fourth Fleet in 1935. Such a propitious (for the meteorologist) analysis from a consistent array of ships has, however, never been repeated. Meteorologists have therefore been forced to develop special analysis techniques to derive information on the surface wind characteristics of typhoons. Myers (1954(a) analysed data from observing network in and around Lake Okeechobee on the Florida Peninsula and examined a number of historical Atlantic Hurricanes, as did Graham and Hudson (1960). Krueger (1959) composited ship observations from six Atlantic hurricanes and Johnson (1954), Myers (1954b), Hubert (1955, 1959), Malkin (1959) and Miller (1963, 1964) examined the surface wind field changes at landfall. These observations were combined into synoptic models of the surface wind field by Myers and Malkin (1961) and Chow (1971).

The most detailed analyses of the surface wind structure in tropical cyclones has been provided by Powell (1982) for Atlantic Hurricane Frederic (1979) and by Holland and Black (1983) for Southwest Pacific Hurricane Kerry (1979). Both studies used data from all available sources, including: aircraft reconnaissance, ships, automatic weather stations on coral cays and reefs, oil rigs, etc. These were reduced to a common level (10m for Powell, 19.5m for Holland and Black) using the boundary layer mode of Powell (1980) and composited over short time periods to build up a picture of the overall structure.

Powell's analyses of Hurricane Frederick over the ocean and at landfall are shown in Figs. 5.3.3 (1) and 5.3.3 (2). Over the ocean the maximum inflow, and maximum wind speeds, were located in the right front quadrant. Shapiro (1983) has suggested that this feature is a result of interactions between the moving cyclone and the underlying surface. To the

southwest the winds were weaker and moderate outflow was present. Such east/west asymmetry has been observed in almost all other studies (e.g. Holland, 1983). Holland and Black (1983) have suggested that this is largely a result of the cyclonic circulation across the meridional gradient in earth vorticity. The earth vorticity is given by the Coriolis parameter, is everywhere cyclonic and increases polewards (in a cyclonic sense). Hence a cyclone in either hemisphere will advect more cyclonic earth vorticity around its western side and less cyclonic earth vorticity to the east. This vorticity advection to the west and convergence to the east, which explains the basic asymmetry in Fig. 5.3.1 (1). Holland and Black further show that asymmetric convective and sea surface temperature fields, combined with interactions between the cyclone and the larger scale environmental flow, may further enhance this effect.

## 5.4 Three-Dimensional Structure

### 5.4.1 Upper level wind fields

There were no upper level wind observations from the cloudy central parts of tropical cyclones until radio-windfinding and aerial reconnaissance were introduced during and just after World War II. Upper winds in hurricanes obtained during this period were analysed by Jordan (1952), Miller (1958a) and Hawkins (1962). These analyses confirmed that in the core of mature tropical cyclones there was a ring of intense cyclonically-rotating winds which extended to just below the tropopause at 16 km or above. Subsequent flights by U-2 aircraft showed that in intense storms this circulation - much weakened - can extend into the stratosphere to 18 km or so (Gentry, 1967; and Koteswaram, 1967).

Izawa (1964) composited winds obtained from Japanese sounding stations during the period 1950-1961 to determine the three-dimensional structure of the wind field in 14 typhoons. He made extensive use of electronic data processing - an early application of these techniques in climatology. Much more detailed studies of tropical cyclones in the northwest Pacific, north Atlantic, and Australia/southwest Pacific regions have been subsequently made by Frank (1977), Gray (1979, 1981), McBride and Zehr (1981), Merrill (1982) and Holland (1983). These studies document a vast range of features of tropical cyclones of different types and characteristics. However, the basic three-dimensional structure of all these systems is essentially the same as that described by Izawa. All typhoons he studied had a substantial northerly component of motion and were located over the sea to the south of Japan between 20°N and 35°N and 125°E and 140°E. To be included in the survey the central pressure of a typhoon had to be below 970 mb. The average of the lowest and highest pressures for each typhoon during the observation period was 925-954 mb. The results of this analysis are shown in

Figs. 5.4(1) to 5.4(4) for selected levels and they define the average wind field out to  $10^\circ$  latitude from the typhoon centre.

The analysis is limited by the fact that it is seldom possible to get a balloon away in winds of 20 m/s or more. Accordingly, the data cannot be taken as describing well the conditions in the outer gale area and beyond. *defining the core region with fidelity. But they can be taken as* Conditions in the core region will be defined later from high resolution aircraft observations.

The distribution of tangential wind at low levels (Fig. 5.4(1)) is seen to be similar to that already given in Fig. 5.3.1(1), the main difference being that the surface winds in the former are over land and have a maximum speed of 20 m/s - less than half of that in Fig. 5.3.1(1) which refers to a level 300 m above the sea. The maximum wind speed at 1 km of 40 m/s (Fig. 5.4(1)) persists up to 9 km and then decreases to only 5 m/s at 18 km. The radius of the 10 m/s isotach contracts with height from  $9^\circ$  lat at 1 km to  $2^\circ$  or  $3^\circ$  lat at 15 km. Anticyclonic flow appears at about  $8^\circ$  lat in the front left of the typhoon at levels above 9 km. By 15 km anticyclonic flow surrounds the cyclonic core which at that level has shrunk to only  $6^\circ$  lat in diameter.

If the velocity of the typhoon as a whole is removed from the wind observations to give the tangential winds relative to the moving centre then some asymmetry in the patterns remains. The vertical cross section of the tangential motion, averaged around the typhoon centre at selected radii (Fig. 5.4(3)) shows that the average tangential wind speed near the centre increases rapidly just above the surface and then remains constant to over 6 km. The anticyclonic flow is seen to be strongest at the 15 km level about  $5.5^\circ$  lat from the storm centre.

Radial velocities are smaller than the tangential components and are more difficult to determine accurately from soundings. They are particularly sensitive to errors in storm position and movement. Nevertheless, a reasonable description of the general pattern was obtained by Izawa (1964). Fig. 5.4(2) shows that the maximum inflow is in the right rear. At 1 km an outflow forms ahead of the centre and persists to great heights although centred more to the right at 3 km and above. The inflow region, by contrast, moves to the left with height. When shown relative to a moving typhoon centre (Fig. 5.4(2) lower) the areas of inflow and outflow change positions so that the maximum inflow occurs at the front of the typhoon with outflow to the rear. The radial flow averaged around the storm at selected radii is plotted as a vertical profile in Fig. 5.4(3). It can be seen that the inflow layer is shallow and that although the main outflow layer is near 15 km some weak outflow is also indicated near 3 km at 10° latitude and more from the centre.

The actual or resultant winds in Fig. 5.4(4) (upper) show the marked spiral inflow of the surface winds but at 1 km the streamlines are more nearly circular. At 3 to 12 km there are signs of an enveloping environmental flow. Above 12 km anticyclone cells appear, mostly to the right of the centre. The relative streamlines Fig. 5.4(4) (lower) indicate a reversed steering flow in the three lower layers. This is essentially due to the strong vertical shear of the environmental steering current in which these storms were embedded. Since the storms largely move with the vertically integrated steering current (section 12) the lower circulation moves faster than the environmental winds there. At 6 km there is very little differential motion but at 12 km there is a tendency for flow through from the rear left to front right quadrants.

Observations from 533 radial flights into hurricanes were used by Shea and Gray (1973) to determine the structure of the inner core region. The winds, determined by Doppler radar, were averaged with respect to the radius of maximum winds (RMW). The tangential winds are shown in plan view for three levels in Fig. 5.4(5). A large degree of asymmetry is indicated for both the actual and relative averages although the relative tangential winds are not quite as asymmetric as the actual winds. Sherman (1956) noted that the difference in speed between maximum winds on the right of a hurricane and those on the left is sometimes two to three times the storm speed. Indeed, observations have been documented of wind maxima occurring in all quadrants, especially for slow moving tropical cyclones (e.g. Powell, 1982; Holland and Black, (1983)).

The actual radial winds (i.e. those winds relative to an instantaneously fixed cyclone centre) obtained by Shea and Gray are shown in Fig. 5.4(6) for the lower troposphere. Most of the inflow takes place in the rear and right quadrants at 900 mb at which level the inward motion is largest in both area and magnitude. At higher levels there are approximately equal areas of inflow in the rear and outflow in the front of the storm centre. Most of this asymmetry cancels when relative flow is considered. However, the relative flow at 900 mb still shows strong inflow to the right of the centre beyond the radius of maximum winds.

When averaged around the centre but with respect to the radius of maximum winds (RMW) the aircraft observations also indicate (Fig. 5.4(7)) that the tangential wind speed falls only slowly with height in the core region retaining 83% of its speed at 6 km. Gray and Shea (1973) found that the vertical shear to 500 mb is negligible (Fig. 5.4(8)). In intense storms the RMW changes little but in weaker storms the strongest winds tend to move towards larger radii at heights above 400 mb (8 km).

with height up to about 250 mb,

In summary, the average wind fields in mature storms show a well-defined low-level inflow and an intense cyclonic core extending to 15 km or more with a surrounding anticyclonic outflow at this level. The outflow in individual typhoons will depend on the broadscale features prevailing in the typhoon's environment. The strong outflow to the north of the typhoon centre indicated in Fig. 5.4(2) may be enhanced because the sample typhoons were approaching upper tropospheric westerlies prior to recurving. The larger amount of information now available on conditions in the upper air around and in tropical cyclones contrasts with both the dearth of observations and the lack of understanding of the wind structure in the lowest one to two hundred metres near the radius of maximum winds. Wind speeds in these low levels form the subject of the next section.

#### 5.4.2 The friction layer

The near surface vertical variation of hurricane force winds in the eye-wall region of a mature tropical cyclone is of importance to both engineers and meteorologists. Unfortunately, the difficulties of observation in such an inhospitable environment have so far precluded the collection of the necessary observations to definitively define this variation. There are reasons for believing that the profile may differ significantly from that in the outer portions of the storm. Fig. 5.4(3) shows that the average vertical shear in the lowest one or two kilometres changes as the core of a typhoon is approached. As air spirals into the storm near the surface it receives injections of momentum from down draughts. However, in the eye-wall region momentum is transferred upwards to great heights and this tends to minimise vertical shear. <sup>Further,</sup> ~~and~~ although there is still dissipation of momentum in a shallow friction layer its precise depth and wind profile are unknown. Note that it is the extreme wind conditions in the core of a tropical cyclone over the ocean as it approaches a coastal community or installation which are of interest to the engineer and meteorologist. It is precisely for these conditions that data are scarce. Profiles in the lesser winds associated with weaker tropical cyclones or mature ones decaying overland are better understood. These will be considered first.

When a wind blows over the ground the effect of friction, which depends on surface roughness, generates turbulent eddies. These in turn reduce the wind speed by an amount which decreases with height up to a level <sup>of a few hundred metres. Above this level is the</sup> ~~of a few hundred metres. Above this level is the~~ "free" atmosphere. The part of the atmosphere in which the influence of surface friction is appreciable is known as the

"friction layer". The theory of turbulence in this region of the atmosphere is very complicated and not yet fully developed, recourse has still to be made to empiricism. Nevertheless, the two current theories of turbulence - eddy coefficient theory and similarity theory - both indicate that, under the same assumptions of horizontal homogeneity, steady state conditions, and constant heat flux and stress, the average wind speed  $\bar{v}$  should vary with height  $z$  above the surface according to the logarithmic relationship

$$\bar{v} = \frac{\bar{v}_*}{K} \ln \left( \frac{z}{z_0} \right) \quad (5.4(1))$$

where  $v_*$  is the friction velocity (equal to the square root of the stress or momentum flux divided by the density) and  $K$  is Von Karman's constant. There are doubts about the constancy of  $K$  but it can here be taken as having the value 0.4. The symbol  $z_0$  is a length characteristic of the surface and is known as the "roughness length". It turns out to be a few per cent of the size of the roughness elements. Typical values are given in Table 5.4.2(1). Over very rough terrain such as in forests and cities it is not clear which is the "surface" from which  $z$  should be measured. The answer cannot be decided theoretically but only from measurements which show <sup>from</sup> which level,  $z_d$ , the wind profile is logarithmic. This level is often called the "zero plane" and represents the effective level of the momentum sink, its elevation  $z_d$  being called the "zero plane displacement". Eqn (5.4(1)) then becomes

$$\bar{v} = \frac{\bar{v}_*}{K} \ln \frac{(z - z_d)}{z_0} \quad (5.4(2))$$

This profile indicates that the rate of change of wind speed with height is greatest just above the level  $z_d$  and that the effect of surface roughness ( $z_0$ ) is not to affect the shape of the wind profile but only its origin and the mean velocity at any given level. The ratio of the wind  $\bar{v}$  to that  $\bar{v}_1$  at another level  $z_1$  is

$$\frac{\bar{v}}{\bar{v}_1} = \frac{\ln [(z - z_d)/z_0]}{\ln (z_1 - z_d)/z_0} \quad (5.4(3))$$

There are problems in applying eqn (5.4(3)). It is difficult to be precise about the value to be allocated to  $z_0$ , because it depends on the shape and distribution of the roughness elements, on the fetch of the wind and on the atmospheric stability. It is normal to specify  $z_0$  for neutral stability. The values in Table 5.4<sup>2</sup>(1) are only approximate. They have been found to change at a given location with change of wind direction and the state of the surrounding vegetation, amongst other things. Additionally, it is not clear where to place the zero plane. A rough rule is to place it at three quarters of the height of the trees or buildings. Notwithstanding these difficulties meteorologists prefer to use this "logarithmic" profile because it has a theoretical basis, whereas engineers usually show a preference for the empirical "power law" profile

$$\frac{\bar{v}}{\bar{v}_1} = \left(\frac{z}{z_1}\right)^a \quad (5.4(4))$$

where  $\bar{v}$  is the mean speed at height  $z$ ,  $\bar{v}_1$  is the mean speed at some reference level  $z_1$  and "a" is a constant. The reference level  $z_1$  can be the standard anemometer height of 10 m, the top of the friction layer, if known, or some other level. In rough terrain the equation can be modified to include a zero plane so that

$$\frac{\bar{v}}{\bar{v}_1} = \left[\frac{(z - z_d)}{(z_1 - z_d)}\right]^a \quad (5.4(5))$$

However, problems again arise in choosing values for  $z_d$  and the empirical constant "a".

Many observations in temperature latitudes over flat open country and over water have yielded values for the power-law exponent "a" from 0.10 to 0.17. The average value of 0.14 is widely used and is sometimes called the 1/7th power law. Over rough treed country and in cities an exponent close to 0.2 (the 1/5th power law) is often found although higher values up to 0.41 have been determined in some experiments over large cities. Helliwell (1971) found an exponent of 0.19 in central London from wind speeds measured atop the Post Office Tower at 195 m above street level and others measured at 61 and 43 m. The general level of roof tops was about 25 m. The zero plane displacement  $z_d$  was found to be 32.5 m which was above the roof tops. Physical reasoning would put  $z_d$  below roof top level - a result obtained when the logarithmic law was fitted to the observations. The computed value of  $z_0$  for the logarithmic profile was 0.7 m.

There are a number of other towers which support instruments to determine wind profiles. Observations in tropical cyclone conditions from towers in the U.S.A., Japan and Hong Kong have appeared in the literature. Observations from the tower at the Brookhaven National Laboratory (18 km inland on Long Island 10° 50'N, 72° 50'W) in hurricane Donna (1960) and from the Tokyo Tower during the passage of three typhoons in 1964 are shown in Fig. 5.4(9). These 10 to 15 min average winds fit a logarithmic profile quite well and indicate values of  $z_0$  between 1.21 and 2.07 m and values of  $v_*$  from 1.46 to 2.16 m/s.

## 5.5 Maximum Winds

### 5.5.1 The Maximum Wind Region

As has been discussed in section 5.3 the maximum winds in tropical cyclones occur in a radial band near the centre and just above the boundary layer. This is a direct consequence of the warm core of these systems (section 4.6.7) which maintains decreasing cyclonic winds with height.

Large variations may occur in the intensity and extent of this maximum wind belt. The radius to maximum winds may vary from 5 to more than 100 km. As shown in Fig. 5.5.1(1) there is a tendency for stronger winds to occur with smaller radii of maximum winds, but there is considerable scatter in individual cases. There is also a slight correlation with latitude (smaller eyes occur at lower latitudes), but again considerable scatter occurs. The maximum wind belt often decreases during the intensification stage and may undergo dynamic oscillations (Shapiro and Willoughby, 1982; Willoughby et al, 1982). When these occur, a secondary wind maximum forms outside the primary maximum wind belt, which then dissipates. As a result the cyclone temporarily weakens, then reintensifies at the new belt of maximum winds contracts inwards.

The structure of this maximum wind belt is also highly variable. As has been noted in section 5.3, considerable azimuthal asymmetry occurs, especially in weaker, rapidly moving cyclones. In a radial profile, the maximum winds may also occur at a sharp, easily defined belt; or they may be spread over some tens of kilometers with no clear maximum wind radius.

This occasional imprecision in defining a maximum wind radius from wind observations is considerably exacerbated when other methods, such as radar or satellite analyses, are used. As may be seen in Fig. 5.5.1(2) the maximum winds typically <sup>lie</sup> ~~be~~ outside the radar eye. The extent varies inversely with intensity, but individual observations are scattered over a range of 60 km.

Classically, most methods have concentrated on determining, or estimating the maximum wind. These are described in the following sections. In using these results, however, the potentially destructive consequences of the above uncertainties and variabilities should be kept in mind.

#### 5.5.2 Central Pressure/Maximum Wind Relationships

Tropical cyclone intensity can be defined by either central pressure or maximum winds, or both. Because wind observations are more ambiguous and less accurate than pressure observations under cyclone conditions, most analysts prefer to determine or estimate the central pressure directly, then use this to indirectly estimate the maximum wind speed.

This maximum wind estimate may be made by fitting an analytic profile, such as described in section 5.3.1, to observed pressures in the cyclone vicinity and making due adjustment for motion and other asymmetries. Alternative<sup>ly</sup> a climatological relationship, such as given by Dvorak (1975)

may be used. But the most popular method is to use an empirically modified form of the maximum cyclostrophic wind equation 5.3.1(8):

$$V_m = C (p_n - p_c)^x \quad (5.5.2(1))$$

where  $v_m$  is the maximum wind,  $p_n$  and  $p_c$  are the environmental and central pressures, and  $c$  and  $x$  are empirically determined constants.

The first use of this technique was by Takehashi (1939), who set  $x = 0.5$  and  $p_n = 1010$  mb and empirically estimated  $c = 6.8$  (for  $V_m$  in m/s) from island observations in typhoons around Japan. Subsequent alternative estimates have been made by Myers (1954), Fletcher (1955), Kraft (1961) and Fujita (1971). An equation with empirically determined  $x = 0.64$  and  $c = 3.4$  has also been developed from very carefully chosen wind observations in the northwest Pacific Ocean by Atkinson and Holliday (1975).

The relation between these different estimates, and their ability to estimate observed maximum winds, are shown in Figs. 5.5.2(1) and 5.5.2(2). The Myers' equation was derived directly from Eq. 5.3.1(8) with  $\beta=1$ . Holland (1980) has shown that this figure is too low and this is substantiated by the generally low estimates in Fig 5.5.2(1). Fletcher's equation was derived from observations over Lake Obeechobee, Florida, but mistakenly used mph directly as kts (Myers, 1954). As a result this equation tends to overestimate the maximum wind speed. The Kraft, and Takehashi equations are essentially the same and provide

reasonable estimates in the north Atlantic. But they overestimate most northwest Pacific typhoons. Here Atkinson and Holliday's relation works best. Fujita's variable relation simply allows a selection of the best fit to any range of observations in any region.

### 5.5.3 Extreme Wind Observations

Maximum wind observations in the most intense typhoons are notoriously difficult to obtain. Meteorologists in reconnaissance aircraft flying at an altitude between 1 and 2 km have reported surface wind speeds in excess of 100 m/s. But these are subjective estimates based on the sea state. More reliance can be placed on the instrumentally determined flight level winds which have been reported in excess of 90 m/s (Table 4.?). In typhoon Ida (1953) a routine reconnaissance flight measured wind of 95 m/s (Jordan, 196 ?). One hour later a U2 overflew the storm and took a series of short interval photographs which Fletcher et al (1961) used to estimate the surface wind speeds at an average 115 m/s and with localised maxima of 122 m/s. In 1969 US reconnaissance aircraft measured mean low level winds of 80 m/s in hurricane Camille but were unable to penetrate the maximum speed region. All anemometers in Camille's path were completely destroyed, but Simpson et al, (1970) estimated that the observed structural damage required surface winds near 100 m/s.

Indeed, very few anemometers survive winds greater than 64 m/s. An anemometer on Tates Cairn (elevation 568 m above m.s.l.) in Hong Kong

recorded a corrected gust of 82 m/s in typhoon Wanda (1962) when the centre ( $p_0 = 942$  mb) was 25km to the south. Sustained 10 minute winds of 74 m/s and gusts of 88 m/s have also been recorded in Japan. Other extreme surface gusts from around the world are shown in Table 5.2(3). *ell*

The maximum possible intensity of a tropical cyclone is difficult to estimate. Central pressures as low as 874 mb have been observed in typhoon Tip (Dunnavan and Diercks, 1980), and Miller (1958b) indicated that 860 mb was possible. Sustained winds of over 100 m/s and gusts near 125 m/s should also be well within the realms of possibility. As shown in the following section, these subjective estimates can be quantified with the use of statistical techniques.

## 5.8 Winds and engineering design

When estimating the effects of typhoon winds on structures the engineer has to consider not only the extreme dynamic pressures and the spectrum of turbulence but also various aerodynamic shape effects. Among these are the distribution of pressure (and suction) on the building surfaces, the increased winds which occur around the corners of high-rise buildings, the disturbance of the flow - acceleration and/or turbulence buffeting - which can arise from large adjacent structures, the "galloping" of transmission lines, "singing" of wires, transverse oscillation of cables and the vibration of tall chimneys etc. The oscillation and subsequent break-up of the 853 m main span of the Tacoma Narrows Bridge at Puget Sound in November 1940 in a mild gale of about 18 m/s is a well known example of an aerodynamic effect. The failure of two large concrete cooling towers 114 m high and 13 mm thick at the Ferrybridge power station in England during a gale on 1st November 1965 is an example of enhanced wind forces due to adjacent towers. On this occasion the one minute mean wind speed at 10 m was close to 23 m/s while at the top of the towers it was 34 m/s.

When air is brought to rest by impacting on an extended surface the kinetic energy of the moving air is converted to a "dynamic pressure  $q$ " in accordance with the formula

$$q = \frac{1}{2} \rho v^2 \quad \text{N/m}^2 \quad (5. \quad )$$

where  $v$  is the instantaneous undisturbed wind speed in m/s,  $\rho$  is the mass density of the air and has a value of  $1.225 \text{ kg/m}^3$  at standard conditions but may be 10% lower in the low pressure and relatively high temperature conditions in typhoons. However, this reduction of density is partly offset by the water content in heavy rain (Faber and Bell 1963). It is therefore usual to use the standard value of mass density for calculating pressures on structures so that

$$q = 0.613 v^2 \quad \text{N/m}^2 \quad (5. \quad )$$

The dynamic pressure exerted at any point on the surface of a body is given by

$$p = C_p q \quad \text{N/m}^2 \quad (5. \quad )$$

where  $C_p$  is a "pressure coefficient" whose value depends on the geometry of the body and local flow conditions. These coefficients have been determined experimentally for many shapes and conditions and are given in tables. Some of the coefficients will be negative and some positive (Fig. 5 ) so that the total resultant forces on the body will be obtained by vectorial summation of the loads on all surfaces. However, the total wind load  $F$  on a body as a whole can also be obtained by using a "force coefficient  $C_f$ " if one can be found in engineering tables for the particular shape and aspect of the body or structure concerned. The total wind load  $F$  is then given by

$$F = C_f q A \quad \text{N} \quad (5. \quad )$$

where  $A$  is the effective frontal area of the body in square metres.

The Aeolian tones from wires in a wind are well known. The pitch rises with wind speed and this effect is used by pilots as a guide to the airspeed of gliders with wire stays. Although the tones from a breeze blowing through pine needles can be soothing, the screech from trees and wires in typhoon winds is deafening and people fighting for their lives in these high winds become acutely sensitive to the variations in pitch which accompany changes in wind speed. The Aeolian note emitted by a wire is independent of its tension but the volume of sound will increase if the tone is close to the natural frequency of oscillation of the wire. The note is caused by the shedding of staggered Kármán vortices (Fig. 5.8 (1)) alternatively from each side of the wire which may itself remain stationary. If  $n$  is the frequency (Hz) of an Aeolian note and  $D$  is the diameter (m) of the wire, branch or string and  $v$  the wind speed (m/s) then, as shown by Strouhal in 1878, the relationship between the quantities is

$$\frac{nD}{v} = 0.21 \quad (5. \quad )$$

The quantity  $n D/v$  is known as the "Strouhal number" and is inversely related to the drag coefficient. The number is appropriate for cylinders and is only constant when the flow is such that the "Reynolds number" is greater than about 500 and less than about 5 000. Reynolds number ( $Re$ ) is given by

$$R_e = vD\rho/\mu = vD/60 \times 10^{-3} \quad (5. \quad )$$

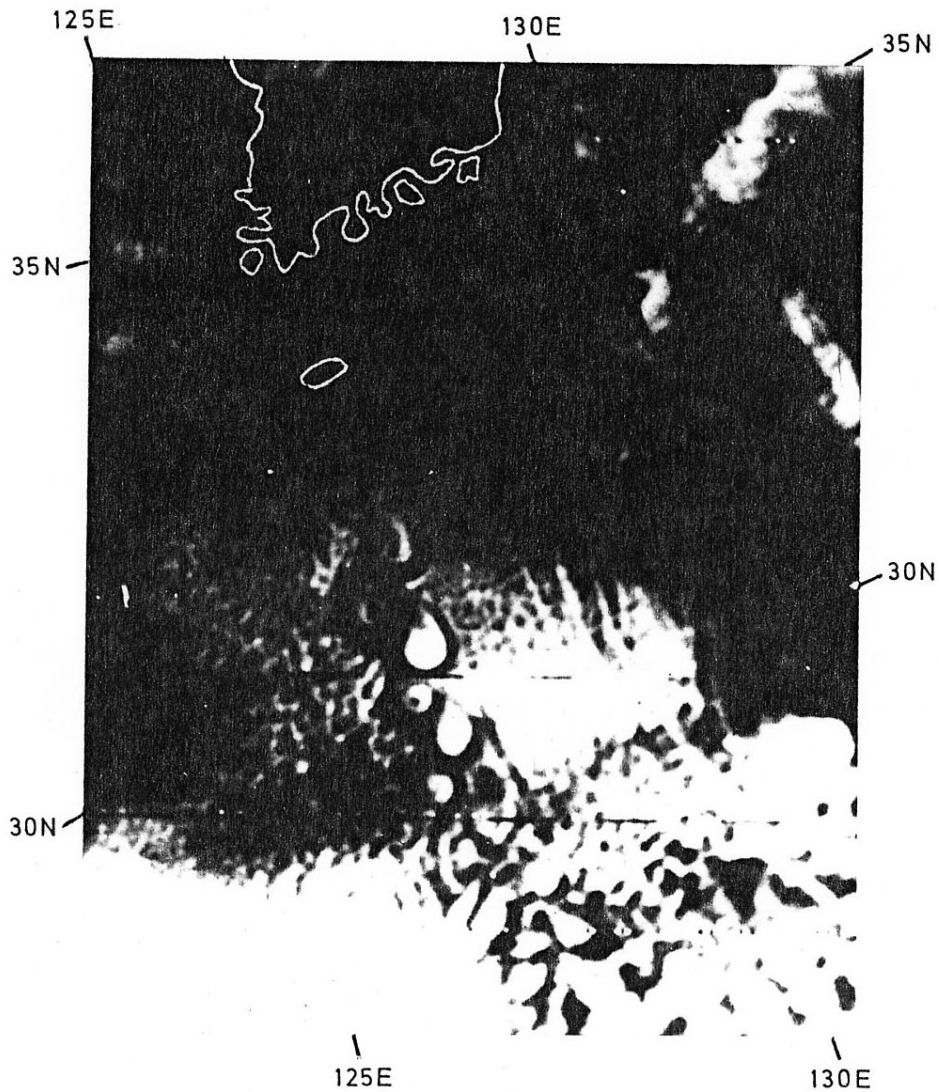


Fig. 5.8 (1). A von Karman vortex street extending about 700 km downwind from Cheju island ( $32^{\circ}33'N$ ,  $126^{\circ}30'E$ ) south of Korea. The island is approximately conical with base diameter  $\sim 70$  km and height 1.95 km. Its effective diameter for vortex shedding is  $\sim 20$  km. This image was received at Hong Kong at 0124 GMT on 5 March 1969 from the satellite Essa 8. The wavelength or spacing between similar vortices is 93 km, equivalent to a frequency or shedding rate of about one each 2.5 h at the prevailing wind speed of about 12 m/s at 1 km.

where  $\rho$  the mass density and  $\mu$  the kinematic viscosity have values of  $1.11 \text{ kg/m}^3$  and  $1.84 \times 10^{-5} \text{ N s / m}^2$  respectively. From eqn (5. ) a wire of diameter 3 mm in a wind of 30 m/s would generate a note (shed vortices) with a frequency of 2.1 kHz. Anemometers have been based on the principle of measuring the frequency of the notes emitted by a cylinder of known diameter.

A cylinder will cease to shed vortices when  $Re$  falls to a value around 50. There is therefore a wind speed below which tones will not be generated. For  $Re = 50$  the critical speed will be

$$v_c = 0.83 \times 10^{-3} / D \quad \text{m/s} \quad (5. )$$

which for a 3 mm wire will be less than 1 m/s. At high wind speeds wires will be in considerable tension and lower pitched natural vibrations will also be heard. From eqn (5. ) a wind of 50 m/s would produce a note of about 100 Hz from a bough or tree trunk 100 mm in diameter. Sustained sound levels in hurricane Camille were estimated at 100 dB (Simpson et al 1970) an intensity of sound greater than that produced by a heavy four engined jet taking off. However, no general noise spectrum can be given for such conditions as the sounds depend on the number and type of trees, wires poles etc. in the area.

In atmospheric flow patterns such as those shown in Fig. 5.8 (1) Reynolds numbers of the order  $10^{10}$  follow from eqn (5. ). However it is found that on this scale the molecular or kinematic viscosity  $\mu$  should be replaced by an eddy viscosity  $K_v$ , for it is the eddies which are primarily responsible for the transport of momentum at this scale. The values of  $K_v$  are found to vary greatly according to atmospheric conditions but a value of  $1.6 \times 10^3 \text{ m}^2/\text{s}$  is typical and also applicable to the conditions in Fig. 5.8 (1). The vortices move downwind at about 75% of the mean wind speed.

The cyclic lateral force on unit length of a wire or other cylinder - e.g. a chimney - due to vortex shedding is equal to

$$C_L \rho \frac{v^2}{2} D \quad \text{N} \quad (5. )$$

where the lift coefficient  $C_L$  usually lies between 0.6 and 1.1. The humming and violent vibrations of an anemometer mast in typhoon winds are governed by eqns (5. ) and (5. ).

4

There are, of course, many other effects of winds which an engineer has to consider. The problems of repeated high loadings which may result in fatigue damage, foundation settlement, excessive deflection and induce motion in tall buildings that may cause nausea or anxiety have been discussed by Davenport (1967). Additionally, it is often necessary to look beyond the static forces and responses involved and consider dynamic effects. As in aeronautical engineering it is possible, given the spectrum of turbulence in typhoon winds and the response of the building to forces of various frequencies, to determine the dynamic response of the building to typhoon winds. We will not go this far here, but some understanding of the design for static wind loading will be given in the following paragraphs.

### 5.8.1 Winds and Buildings

Typical flow patterns of the wind around a building are shown in Fig. 5.1 pressures above atmospheric are experienced on the front of the building while a partial vacuum is formed in the rear. Suction effects are also experienced where the flow is accelerated or separates from the building such as over the roof or at corners. This effect is most marked on windward edges. The lower part of Fig. 5.2 shows the readings of a surface pressure gauge at a point on the roof of a house. It will be seen that the pressure at this point is not steady but fluctuates in a random manner about some mean value. The pressure at a point is more variable than the speed of the oncoming wind because of the eddies induced in the flow by the building. These eddies form, dissipate and re-form causing pressure fluctuations to come in bursts. Fig. 5.3 shows that the average pressure at the gauge is negative, that the maximum departures are in the negative (suction) direction and that they greatly exceed the mean. The figure illustrates the necessity of considering loads of several times the mean on small building details and cladding.

Fig. 5.3 shows concrete slabs lifted by suction at the windward edge of a roof. Note that the effect is markedly worse on the windward edge and that in the mid-section of the roof the porch probably assumed the role of a windward edge and bore the severest action so sparing the tiles further down wind. The house in Fig. 5.4 was in an area of general devastation. The roof on this modest building remained intact probably because the <sup>roof</sup> ventilators helped to equalise the pressures inside and outside the building. Farmer's houses near the coast of South China often have wires or ropes swung over the roof with large rocks hanging on either end, to help resist the lifting forces in typhoons.

The mean wind causes high rise buildings to deflect to an equilibrium position whilst swaying about this position in accordance with their natural period of vibration and the wind fluctuations. The natural period of a building may increase with increasing wind speed (as in the experimental building of sect 5. ) due to a change in its stiffness with deflection. It is found that the mean response increases if stiffness decreases and the dynamic response increases with an increase in the natural period. The Empire State Building in New York has a natural period of

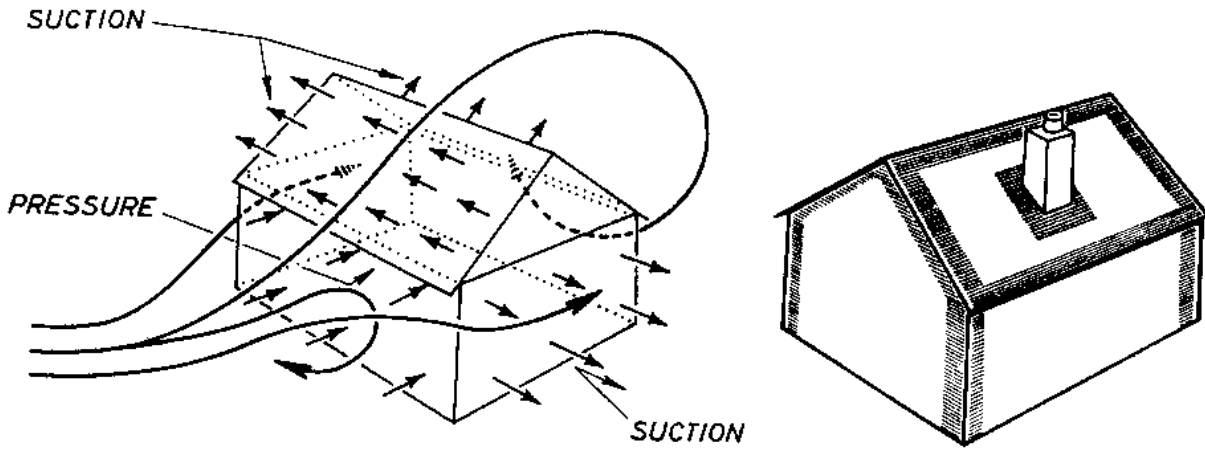


Fig. 5.1. On the left is shown a typical flow pattern and the areas of pressure and suction around a building with a gable roof. On the right are shown areas where suction must be allowed for on the cladding. (After Marshall 1977).

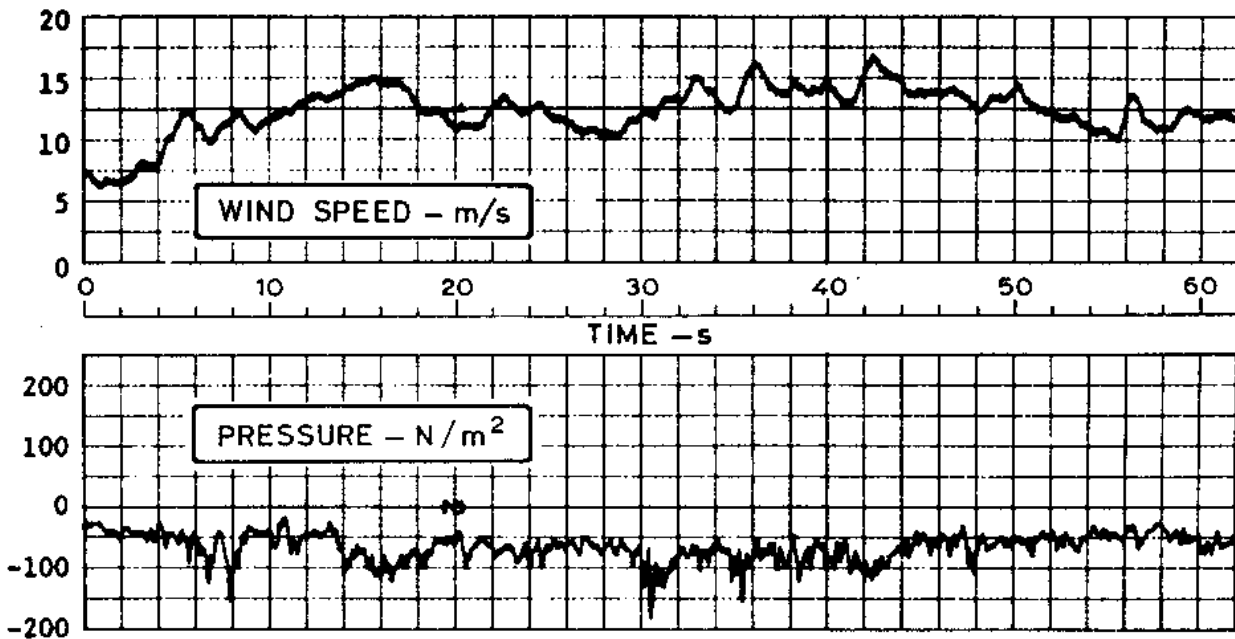


Fig. 5.2. A typical record of wind speed and pressure at a point on the roof of a house (After Marshall 1977).

oscillation of about 8 seconds, smaller high rise buildings have shorter periods of the order of 1 to 5 seconds. People begin to notice the sway of a high building when the acceleration involved is between one to ten thousandths of that due to gravity. In a 40-storey building with a 4 second natural period of vibration these accelerations would be reached when the sway amplitude amounts to 4-40 mm. (See sect 5. )

The distribution of pressure due to the wind on a high rise building can be simulated in a wind tunnel on the assumption that the building and the model can be considered as flat plates or bluff bodies for which the flow patterns are independent of Reynolds number. The Reynolds number (eqn (5. ) replacing  $d$  by  $\lambda$  <sup>found from  $\lambda$  by the building height 2)</sup> in wind tunnels is usually in or near the range  $10^4$  to  $10^5$  which is only about one hundredth of typical full scale values. Nevertheless, this is well within the region in which flow around a flat plate, mounted normal to the direction of the flow, is unaffected by changes in Reynolds number. Indeed, provided that the topographical features, including individual buildings within a few hundred metres and the mean wind profile are correctly reproduced in the tunnel it transpires that realistic results can be obtained. Since about 1960 a number of laboratories have used wind tunnels for estimating not only the pressure distribution on an individual building but also to determine the effects due to adjacent buildings, and the speed of the wind round corners, through archways and in courtyards etc. // Fig. 5.5 shows the average pressure over the surfaces of model of a high rise building as obtained in the Building Research Establishment tunnel in England. The pressures are expressed as conventional pressure coefficients by dividing by the dynamic pressure of the wind at roof level. Positive coefficients indicate areas of above atmospheric pressure and vice versa. When  $C_p = 1$  the full dynamic pressure  $q = \frac{1}{2} \rho v^2$  is attained. On sidewalls, roof and leeward walls, which experience suction, the average pressure coefficient  $C_p$  may be as low as -2.0. <sup>(Penwarden and Visk 1975)</sup> The air flows in a direction perpendicular to the surface-pressure contours so that, for example, the flow from the high pressure centre (0.7) will be upwards to the roof and outwards to the sides. It is such flows as these that cause streams of rain water on windows to apparently defy gravity during the <sup>passage</sup> height of a typhoon. x

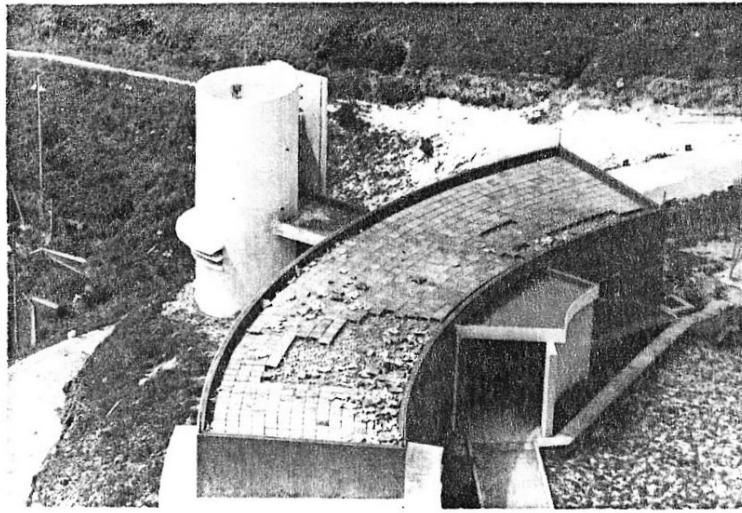


Fig. 5.3 . Damage to concrete tiles on the roof of a building at Tate's Cairn, Hong Kong caused by winds associated with typhoon Wanda 2 September 1962. Peak gust speeds at the nearby radar station attained 84.5 m/s. (Peterson and Cheng 1966.)



Fig. 5.4 . An old building with roof intact after the passage of typhoon Wanda 1962 at Hong Kong. Retention of the roof was probably due to the equalisation of pressure through the ventilators on the eaves. Note lack of leaves on the trees and debris - either wind or water borne - on the tree at right. (From Peterson and Cheng 1966.)

## Roof

### -0.5

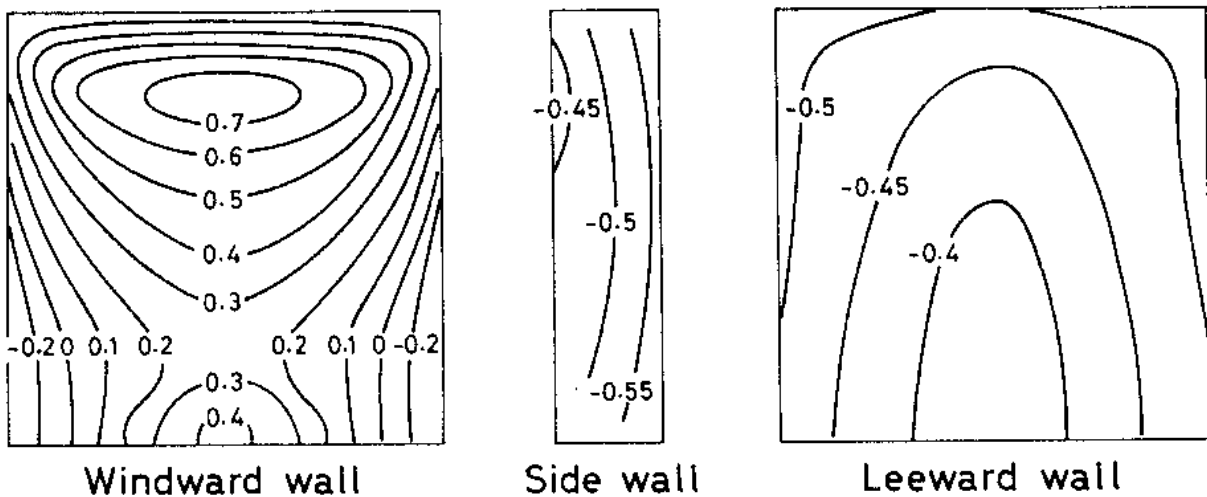


Fig. 5.1. Typical pressure distribution on the surfaces of a model building of height 0.4 m and width 0.4 m, with a low building 0.3 m upwind. Pressures are expressed as coefficients,  $C_p = (p - p_o) / \frac{1}{2} \rho v_z^2$ , where  $p$  is the pressure at the surface,  $p_o$  is the static pressure in the wind tunnel airstream,  $\rho$  is air density,  $v_z$  is the wind speed at building height  $z$ , and  $\frac{1}{2} \rho v_z^2$  is the dynamic pressure of that wind at roof level. (From Penwarden and Wise, 1975.)

The almost complete destruction of Darwin on Christmas Day 1974, Fig. 5. illustrates the importance of both estimating accurately the extreme winds at a location and enforcing an appropriate building code of practice.

### 5.8.2 The design wind speed

The extreme wind speeds to be used for the rational design of structures are usually specified in the appropriate national or local building code and standards. There are great variations in the specifications contained in these codes especially for those areas subject to tropical cyclones (Faber & Bell 1963). It is usual to assess a "basic wind speed" at 10 m for the site and then to modify this to obtain a "design wind". Some codes specify how the basic wind speed should be chosen, others simply state its speed. Some codes vary the basic wind to match the exposure of the site. Most codes - but not all - specify how the wind should change with height, some maintain a constant wind speed others use a power law - usually with exponent 0.14 - others, specify the wind loadings for design in certain height ranges. For example, the uppermost of the six ranges in the Hong Kong (1975) Code specifies a constant design pressure of 4.3 kPa above 140 m. Some codes relate the design wind speed to the type of building. The American National Standard A58, for example, specifies that a basic wind speed corresponding to a 50-year mean recurrence interval should be used for all permanent structures except those involving a high degree of hazard to life and property in case of failure, for which a 100-year wind should be used. The code should specify the distribution to be used to obtain the 50- or 100-year wind (sect 5.7). The National Building Code of Canada specifies the use of the type I (Gumbel) distribution whereas the American National Standard A58 specifies both the type II (Frechet) distribution (sect 5.7) and its parameters. The averaging periods for the winds used in the various codes are: instantaneous gust, 2, 3 or 30 seconds and one minute and the variable averaging period associated with the "fastest mile of wind". Some codes specify design wind pressures and avoid mention of a design wind directly, although of course, one is implied.

### .1 Selection of averaging period

If a gust is to completely embrace a structure and so establish the flow pattern and aerodynamic forces appropriate to its speed, then the duration of the gust must have some minimum value determined by its speed and the dimensions of the structure concerned. An instantaneous gust which could establish the full dynamic pressure on a signboard or pylon might be unable to do so on a large building. The building might be embraced by a 5 second average gust which at 50 m/s would have a length of 250 m or so. Anemometers usually used at airports and weather offices have responses of from one to a few seconds and are therefore associated with peak gust speeds averaged over this period. These peak gust speeds are relevant to the design of most buildings. The British Code 1972 (BS. CP3: Chap. V:Part 2) uses as a basic wind speed the 3-second gust speed and includes provision for the use of a factor to make allowances for the effects on buildings of different sizes. The use of gust speeds has the additional advantage that corrections for exposure, surface roughness and variation of speed with height are less than for winds of longer averaging period (sect 5. ). Winds determined over longer averaging periods may, of course, be reduced to short-period equivalents (sect 5. ). At 80 m/s the fastest mile of wind corresponds to an averaging period of about 20 seconds.

### .2 Selection of return period

The return period or mean recurrence interval selected for the basic wind speed depends upon the intended purpose of the building and the consequences of its failure. It is especially important that buildings which hold many people or have a post-disaster function such as hospitals, buildings associated with communications, police stations and schools should be strongly designed and constructed. For such structures

a mean recurrence period of perhaps 1000 years could be used for the basic wind speed depending on an assessment of the risk of failure in relation to the purpose, probable lifetime and cost of the structure concerned.

There is always a risk that wind speeds in excess of the basic wind speed will occur during the expected life of a building. This is illustrated in Table 5. where it can be seen that there is a probability 0.63 that the wind speed associated with a 100 year return period will be exceeded at least once in 100 years. Should the design wind speed be exceeded it does not necessarily mean that the structure will fail.

Table 5. Probability of exceeding a basic design wind speed (From Faber & Bell 1963)

Desired Lifetime N Years	Risk % of exceeding in N years the mean hourly wind speed corresponding to the indicated return periods						
	0.632	0.50	0.40	0.30	0.20	0.10	0.05
Return Period in Years							
2	2.5	3.4	4.4	6.1	9.5	19	39
10	10	15	20	29	45	95	196
20	20	29	39	56	90	190	390
30	30	43	59	84	134	285	585
40	40	58	78	112	179	380	780
50	50	72	98	140	224	475	975
80	80	115	156	224	358	759	1560
100	100	144	196	280	448	949	1950

From this Table it will be seen that there is a 10% risk that the wind speed appropriate to a return period of 475 years will be exceeded in a lifetime of 50 years.

### .3 Determination of wind loading

The procedure usually adopted in good building codes is to first determine a basic wind speed. This wind will be the average over some stated period - preferably 2-3 seconds - and will refer to some stated height - preferably 10 m - and will have been determined to occur for the district concerned about once in, say, 50 years on average. This wind is then adjusted by multiplying it by factors to take account of variables such as topography, ground roughness, building size and height above ground and the degree of security required and the period of time in years during which it will be exposed to the wind (see e.g. British Code BS CP3 1972). In addition, when the extreme winds are attributable to tropical cyclones a factor can be introduced to take account of the reduction of their maximum wind speeds with distance inland from a coastline. If the basic wind has been chosen as a 2-3 second average for the coast then factors of 0.88, 0.82 and 0.78 apply at distances inland of 48, 96 and 144 km (Malkin 1959). The decrease over rough terrain will be more rapid than indicated by these figures. The result of applying the foregoing factors to the basic wind speed yields the design wind speed.

The design wind speed is next used as the basis for estimating the wind loading at different heights on a building. A variety of methods can be used to ensure that gust factors used at different levels to obtain peak pressure loadings are appropriate to both the wind averaging period and the structure concerned. The variation of wind speed with height is dependent on the averaging period, the 0.19 power law referring only to winds averaged over about five minutes or more. It is not our purpose to discuss the many possible combinations of these factors but, as an example of procedure, we can follow Mackey et al (1972) in computing the wind load on a 179 m building in Hong Kong.

Mackey et al determined the one hour mean wind speed with a 50-year return period from the records of a well exposed anemometer on Waglan, an offshore island. These winds were representative of those over the sea at a height of 75 m. The mean hourly wind speed there, with a 50-year recurrence interval, is about 49 m/s as shown in Fig. 5. The power law of eqn (5. ) with exponent 0.19 was used to determine the equivalent 10 m - wind of 34 m/s. This was taken as the basic wind to be used for design purposes. Since the building was to be on the coast near sea level the basic wind needed no further modification for exposure and so became

the design wind. The mean hourly winds at other heights - shown in Table 5 - were determined by using the 0.19 power law. The winds were next converted to dynamic or velocity pressure  $q$  using eqn (5. ) so that, for example, the 10 m dynamic pressure was  $0.71 \text{ kN/m}^2$ . A gust factor was next applied at each level to yield the peak gust pressures which would be associated with that type of building in typhoon winds. From full scale measurements in typhoons at Hong Kong (sect 5. and 5. ) a speed factor of 1.3, yielding a gust-pressure factor of 1.69, was found to be applicable to buildings exceeding 30 m in height. This factor was determined from measurements at 61 m and it could be progressively decreased with height but was kept constant to give conservative figures for the upper part of the building. Both the dynamic pressure  $q$  and the design gust pressures are entered in Table 5.

Table 5. Variation of the design wind and design pressure with height

Height $z$ - m	10	20	30	40	50	100	150	200
Design wind $v$ - m/s	34	38.8	41.9	44.3	46.2	52.7	56.9	60.1
Dynamic pressure $q_v$ - $\text{kN/m}^2$	0.71	0.92	1.08	1.20	1.31	1.70	1.98	2.21
Gust pressure - $\text{kN/m}^2$	1.20	1.55	1.83	2.03	2.21	2.87	3.35	3.73

Fig. 5. <sup>shows</sup> the wind loadings from Table 5 and those computed by two others methods. Curve A is based on the figures in Table 5, whereas the other two are calculated according to the United Kingdom and Hong Kong building codes of practice. For ease of comparison a force coefficient  $C_f$  (sect. 5 ) of unity has been adopted. More information on building to resist typhoon winds will be found in the five volumes of the U.S. National Bureau of Standards Building Science Series 100 (1977). These volumes deal particularly with the design of low cost buildings and homes in those countries in the tropics which are subject to visitations from typhoons.

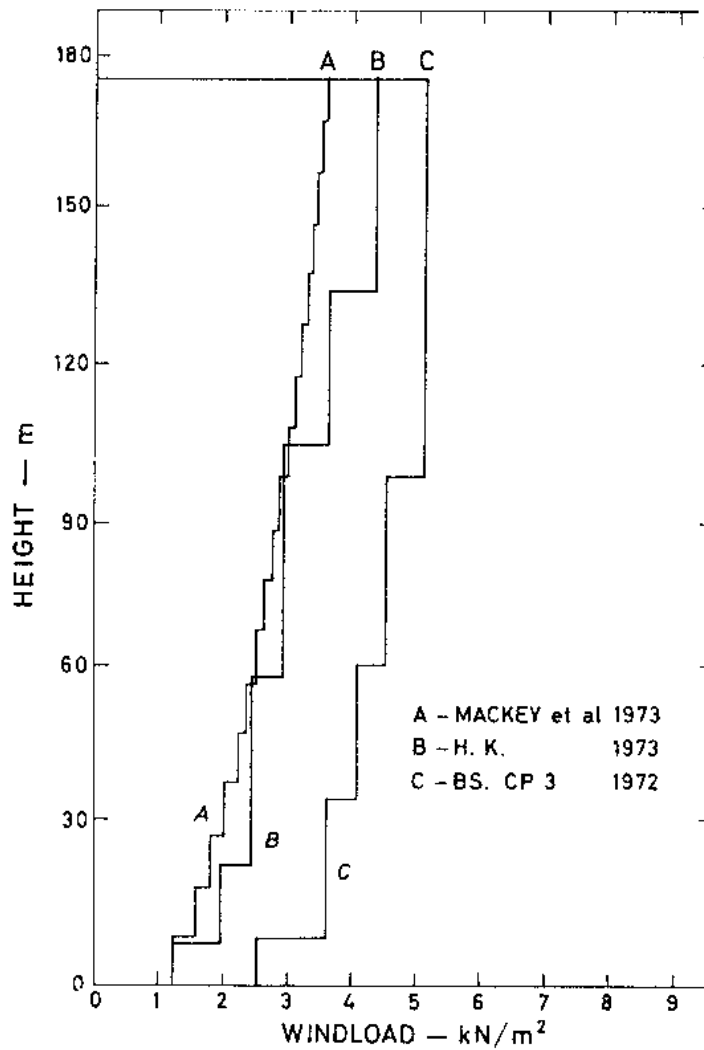


Fig. 5. Comparison of the computed wind loading on a Hong Kong building 179 m high, based on three different building codes of practice. (Amended from Mackey et al 1973.)



Fig. 5. . The ten-storey building at Cape D'Aguilar, Hong Kong which was built to study wind effects. The four 61 m masts carry 20 anemometers.

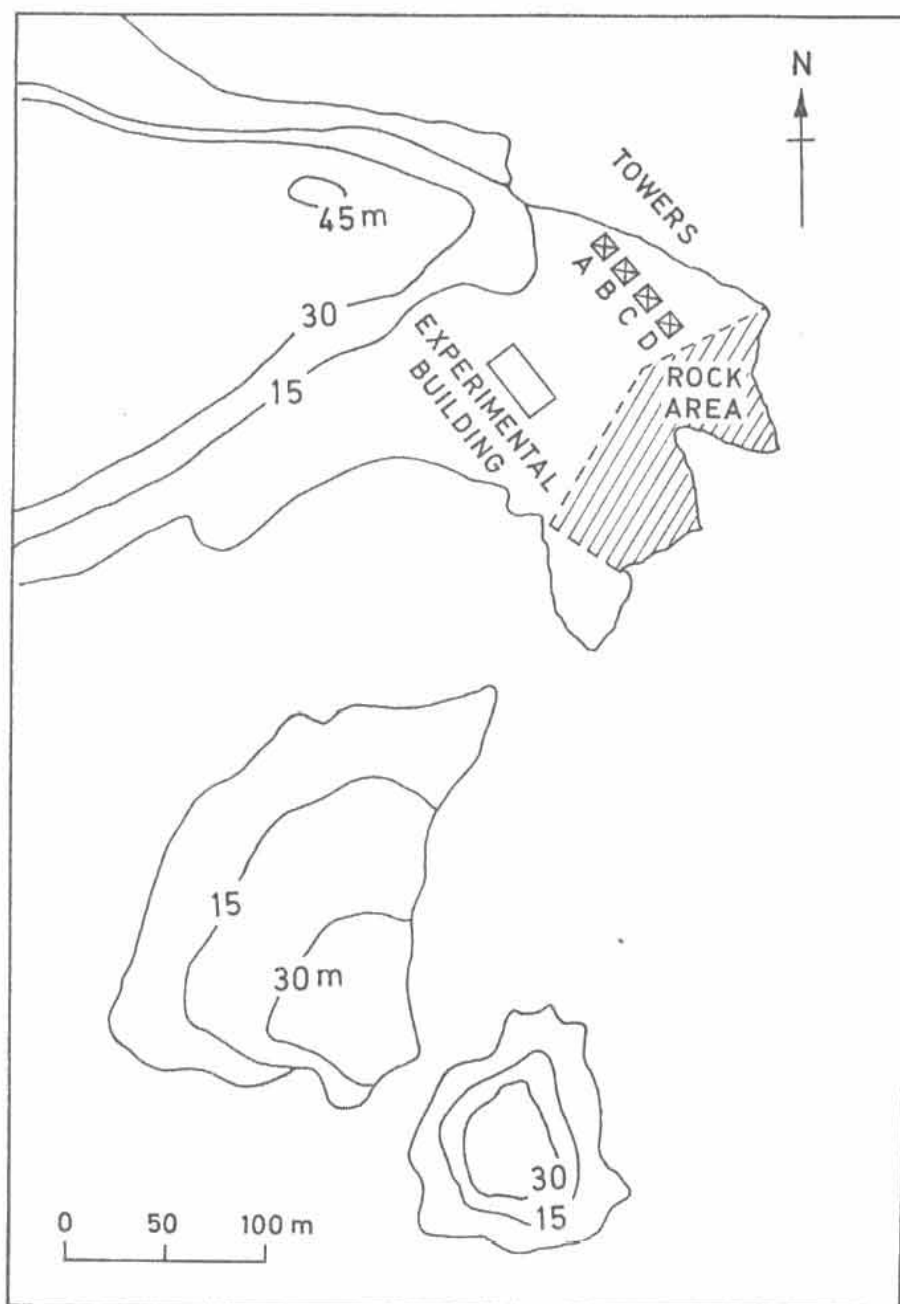


Fig. 5. . Map showing the location of the four anemometer towers and the experimental building shown in Fig.5. .

5.8.3 Measurements at full-scale

Much of our present knowledge relating to wind effects on structures comes from wind-tunnel studies on model buildings, but there are factors which cannot readily be scaled down to model size. The development of lightly-framed, high-rise buildings has greatly increased the need for confirmation that wind-tunnel results can be reliably applied to structural design codes. This can be done by constructing a full-scale, instrumented building to measure the wind effects and then comparing them with those determined on a model in a wind tunnel. One such experiment was started in late 1969 by the Centre of High Building Research at the University of Hong Kong.

Hong Kong is in a region where typhoons are relatively frequent. It was therefore thought to be a good location for such experiments. The building was sited as close to the sea as possible (Fig. 5. ) so that the measured winds and associated pressure effects would be as little disturbed by terrain effects as could reasonably be attained; this facilitates both the analysis and transposition of results. The ten-storey building is of exposed structural steel construction with fully-welded beam and column connexions and curtain-wall glazing on all vertical faces. The building measures 18.3 m x 9.2 m in plan and is 30.5 m high.

The velocity of the wind approaching the building is determined by anemometers at the four levels 12 m, 28 m, 43 m and 61 m above mean sea level on each of the four 61 m masts (Fig. ). The anemometers were of the quick-response type developed at the U.K. Electrical Research Association. In this instrument the force on a ping-pong ball supported by a thin strut is sensed by electrical strain gauges. Each anemometer measures the wind component in one direction only so that two instruments are required to derive wind speed and direction. In addition to the sixteen sets on the masts there were 3 sets between the mast and the building. Four Meteorological Office MK II cup-generating anemometers were also mounted on one of the masts.

The external walls of the building carried 72 flush-mounted pressure cells of the strain-gauge type which were developed at the U.K. Building Research Station. These gauges measure the difference between the external pressure and that within the building. To enable pressures over the building to be compared it is necessary to vent the gauges to a common static pressure. This is done by a system of large diameter pipes leading to the atmosphere at a point distant from the building. Electro-optical tracking instruments were used to record the sway movements and vibration characteristics of the building. Data from all instruments were sampled sequentially at the rate of 10 samples/second/channel. These were time multiplexed, converted to digital form and recorded on 9-track magnetic tape.

So far (1977) no severe typhoon has been experienced in Hong Kong since the experiment began. Nevertheless, much useful material on both wind structure and building response has been achieved in moderate typhoons in which maximum gust speeds of  $\quad$  m/s have been recorded. The results have been presented in many papers and theses.

In light winds the fundamental frequency of vibration of the building was found to be 1.04 Hz but this decreased to 0.90 Hz in winds of 15 m/s and to 0.80 Hz at higher wind speeds (Lam 1971). The top of the building oscillated with an amplitude of about 25 mm.

Fig. 5. shows a spectrum of the pressure variations at gauges near the centre of the windward face of the building in typhoon Ruby (1970). Also shown is the spectrum of the accompanying wind-induced vibrations of the building. The peak of the building response at 0.9 Hz corresponds to the fundamental frequency of the building and occurs in a region where the wind or pressure spectra contain relatively little energy. Because the natural frequency of the building is high when compared to the frequency of the peak in pressure or wind variations (about 0.15 Hz) the response of the building at resonance is less than that due to background excitation. The sway movements therefore tend closely to follow the pressure fluctuations. The correlation co-efficients between simultaneous sway movements and the windward pressure lay between 0.7 and 0.8 whereas the correlation with leeward suctions was only 0.3.

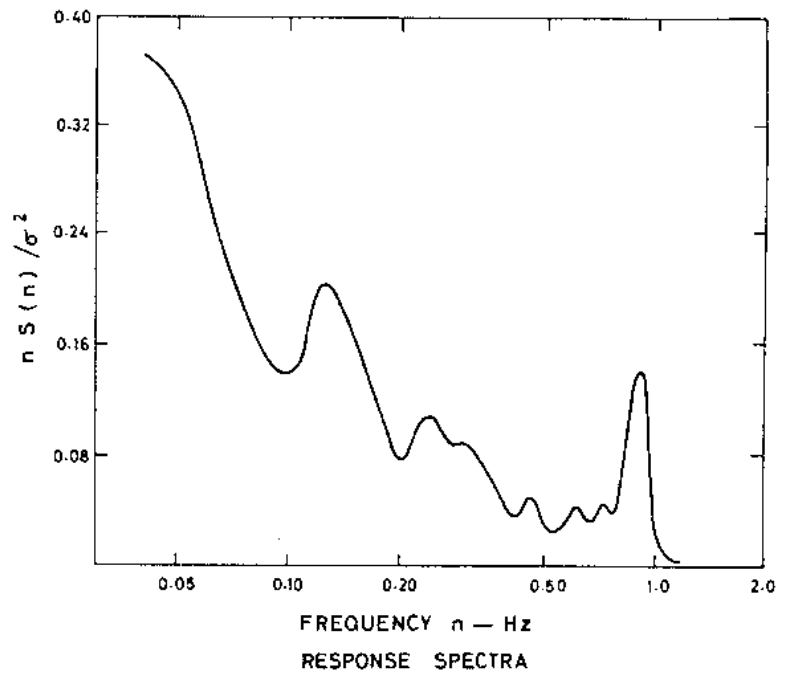
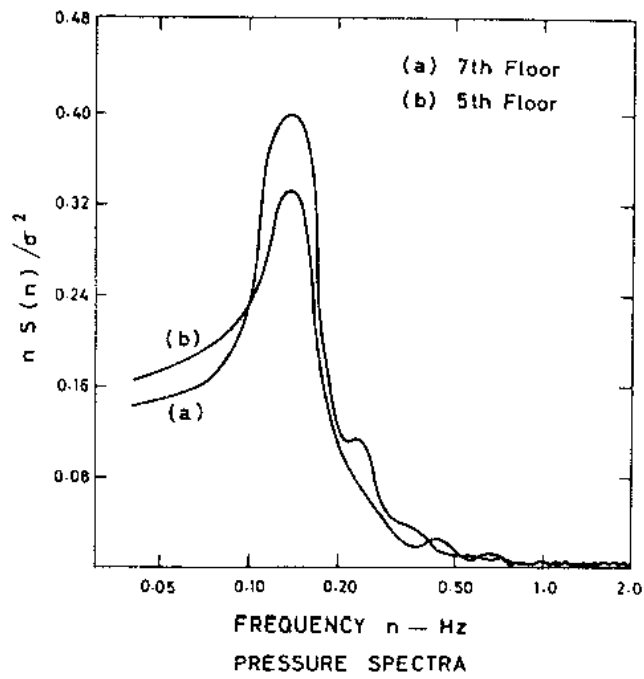


Fig. 5. . A spectrum of the wind pressure variations on the face of an experimental building in typhoon Ruby (1970) and, on the right, the spectrum of the resulting building vibrations. (After Lam 1971)

Using the pressure gauge readings the total force on the building has been measured in several typhoons and compared with wind-tunnel estimates (Mackey et al 1974). Wind tunnels with maximum speeds of about 10 m/s are usually used for building tests and time-averaged winds and forces are measured. When using eqn (5. ) the total force  $F$  will be a time average if the wind velocity used to determine  $q$  is averaged and the value of an appropriate total force coefficient  $C_f$  will be required. Fig. 5. shows the variation of  $C_f$  for the building with averaging time for winds in three typhoons. The authors suggest that  $C_f$  increases with averaging period because the "air cushion" on the windward face of a slab block building absorbs short-duration gusts so reducing the peak loads and also producing pressure pulsations with periods depending on the face dimensions of the building. This effect may account, in part, for the poor correlation between building sway and suction on its lee face.

In order to compare full-scale and wind-tunnel results it was necessary to choose a value of  $C_f$  for the building which would be consistent with the time-averaged wind-tunnel measurements. Fig. 5. shows a 60 second averaging time to give a reasonable estimate of the mean-force coefficient. When this was done it was found that the model tests - with simulated wind profile and environment - predicted the total force to within 2 to 4% of the full-scale values obtained in typhoons Freda (1971) and Lucy (1971).

Mackey et al (1974) point out that building codes on static wind loading invariably specify the use of eqn (5. ) to calculate the total wind load  $F$  due to a maximum gust speed. For this purpose, either a maximum gust speed is used directly or a mean wind is used to determine  $q$  which is then adjusted by applying a gust factor. In either case the force coefficients are obtained from wind-tunnel tests. Thus a mean force coefficient is often used to calculate an instantaneous gust load, a procedure which will only give a correct result if  $C_f$  is invariant with averaging period. In Table 5. measured maximum loads on the building in two typhoons are compared with those predicted by eqn (5. ). In using eqn (5. )  $C_f$  has been taken as 1.1. as recommended in the British (1972) and other codes and the 3-second gust speed at the time of the pressure (loading) measurements is used to determine  $q$ . The

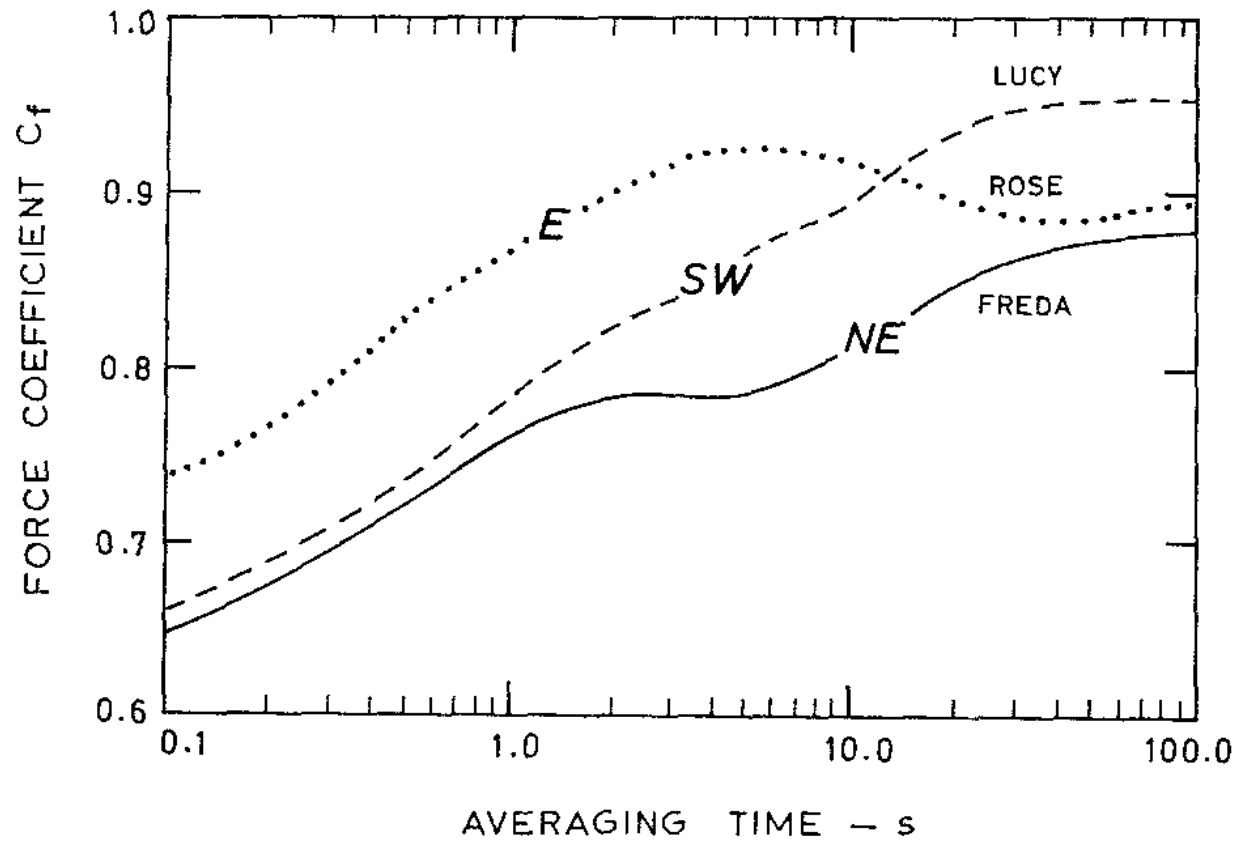


Fig. 5. Variation of the force coefficient  $C_f$  with averaging time in typhoon Lucy, Rose and Freda in 1971. The direction of the wind in each case is indicated. (From Mackey et al 1974)

overestimation of wind loads caused by using the wind-tunnel value for  $C_f$  is seen to be about 28%. Time-averaged loads obtained in a wind tunnel were therefore found to be close to those found in full-scale experiments but the use of wind-tunnel force coefficients overestimates the maximum gust loads.

Table 5. Comparison of measured and predicted wind loads.  
(After Mackey et al 1974)

Typhoon name	Freda (1971)	Lucy (1971)
Measured maximum load over 0.1 s.	212.3 kN	347.2 kN
Maximum 3 s gust	26.98 m/s	34.28 m/s
3 s dynamic pressure, $q$	446.2 N/m <sup>2</sup>	720.4 N/m <sup>2</sup>
$F = C_f qA = 1.1 qA$	273.5 kN	441.6 kN
Ratio of measured to calculated wind load $F$	1.29	1.27

#### 5.8.4 Windows

Windows are particularly liable to typhoon damage. The acute danger to the occupants of buildings from flying glass has already been described (sect ) and to this danger must be added the destruction which rapidly follows the failure of a window frame or window glass. The sudden entry of the wind causes wild flaying of heavy curtains and those which are weighted can be very destructive. Room door locks often fail as the wind rushes into a room and doors may be blown off their hinges. Furniture is blown around and damaged and rapid flooding occurs. If the original failure was due to a faulty catch, the swinging window frame will soon break adjacent windows and hasten destruction. Metal frames are inclined to bend and sometimes bulge sufficiently to release a catch. Additionally, the rattling and vibration of windows with loose catches can soon lead to failure. Large windows bow inwards in a terrifying manner and can sometimes pop out of their frames before breaking. Anxious occupants of rooms watching a bowing window become increasingly apprehensive as they hear the rumble of each approaching gust. In typhoon Wanda 1962 some blocks of new flats on a ridge on the south of Hong Kong island suffered badly from failed window frames which were of aluminum and had bent sufficiently under the wind loading to allow the glass to pop out. Residents were obliged to shelter in the lift wells. People who have experienced a severe typhoon often enquire about the safety of their windows and because of this interest the results of some studies and recommendations in this field are described in the following paragraphs.

It is good practice to set up wooden shutters or stressed wire braces on accessible large areas of glass. Shutters are particularly desirable near street level where flying debris may be encountered. In areas where tropical cyclone passages are expected several times each year this exercise, for large enterprises, can be both costly and a deterrent to business. Other solutions are therefore sometimes sought such as, for example, the fitting of metal shutters which can be moved into position automatically when the wind speed increases or warning signals are hoisted (Fig. 5. ).

Ishizaki (1972) both measured and calculated the deflection of large glass panes under air pressure. In each case pressure was increased until the glass broke. Some of his results are shown in Fig.5 . Saffir (1977) proposed maximum areas of plate glass of varying thickness for use in exterior walls. These are given in Table 5. and are applicable to windows having adequate four side support in which the deflection of the supporting members is not in excess of 1/180 of their length.

Table 5. Recommended maximum area of glass ( $m^2$ ) for design wind speed of 63 m/s\* at 10 m above ground (after Saffir 1977)

Height above ground	Glass thickness (mm)								
	3.2	5.0	5.6	6.4	7.9	9.5	12.7	16.9	19.1
1 m	1.1	2.0	2.5	3.1	4.4	5.6	8.2	11.1	14.0
9 m	0.6	1.2	1.5	1.8	2.6	3.3	4.9	6.6	8.3
27 m	0.5	0.9	1.1	1.4	1.9	2.5	3.6	4.9	6.2
92 m	0.3	0.6	0.8	1.0	1.3	1.8	2.5	3.5	4.4
267 m	0.2	0.5	0.6	0.7	1.0	1.3	1.8	2.5	3.2
over 300 m	0.2	0.5	0.6	0.7	1.0	1.2	1.8	2.5	3.1

\* "Fastest mile of wind" equivalent to a 26 second average:

The equivalent peak gust speed is about 70 m/s.

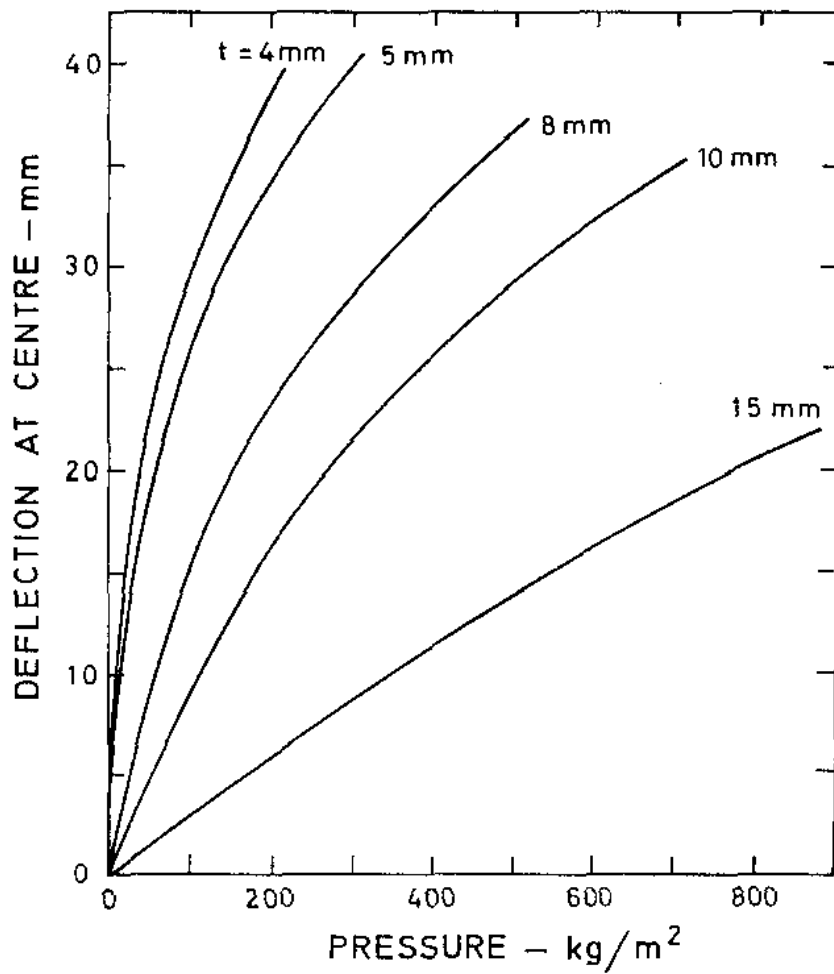


Fig. 5. . Deflection of the centre of sheet glass (thickness  $t=4\text{mm}$ ) and plate glass ( $t=5,8,10$  and  $15\text{ mm}$ ) of size  $2\text{m}$  by  $2\text{m}$ . Multiply  $\text{kg}/\text{m}^2$  by  $9.807$  to express pressure in S.I. units of  $\text{N}/\text{m}^2$  or Pa. (After Ishizaki 1972).

### 5.8.5 Wind and people

#### .1 Body forces

When a wind attains a speed of 10 m/s it is noticed as a force on the body and begins to blow off hats and cause difficulties for those using an umbrella. Noise begins to be generated in the ears. Windspeeds from 10 to 20 m/s progressively impede the progress of pedestrians and gusts cause difficulties with balance. A steady wind of 20 m/s over open country or on the coast is more easily resisted than are peak gusts of the same speed, these cause people to lose their balance and be blown over. High rise buildings can distort the local wind flow and give rise to local winds of 20 m/s when the general wind speed is much less. Penwarden and Wise (1975) examined the circumstances resulting in the death of a pedestrian at the corner of a 16-storey building in Portsmouth, when the free wind was between 13 and 20 m/s with gusts to 25 m/s. From tunnel tests they estimated that speeds at pedestrian level near the building corners would have been in the range from 15 to 24 m/s with gusts to 30 m/s. One such windy spot occurs near the Peninsula Hotel, Hong Kong where it was the practice for the police to run a rope across the road, during typhoon gales, to arrest the flight of pedestrians caught up by the wind. The energy expended in walking into the wind can be expressed as the product of the force of the wind on the body and the walking speed. In Table 5. the muscular activity required for walking into winds of various speeds is equated with that required to walk up hill slopes in calm conditions.

Table 5. Hill slopes and wind speeds which require the same muscular power from walkers. (From Penwarden and Wise 1975)

Slope of hill	1/20	1/10	1/7	1/5	1/4	1/3
Wind speed - m/s	9	13	15.5	18.5	21	24

In tropical cyclones, raindrops begin to feel painful on exposed skin at about 15 m/s and prevent vision to windward at about 20 m/s and above. At hurricane force ( $> 33$  m/s) variations of atmospheric pressure in gusts cause sensations in the ears and on the chest and give rise to feelings of nausea in many people.

## .2 Vibration tolerance

The vibration of buildings during high-wind conditions (sect 5 ) can cause occupants to experience nausea, fear and pain. The particular sensation or combination of sensations produced depends on both the amplitude and the frequency of the vibrations. For instance, a vibration with a displacement amplitude of 20  $\mu\text{m}$  at a frequency of 5 Hz is just perceptible, but it becomes painful if the frequency is increased to 50 Hz. The threshold of perception corresponds to a peak velocity of 0.3 mm/s, and a vibration will be considered annoying if the velocity exceeds 2.5 mm/s. Dieckmann made observations on the effects of vibrations on human comfort. His results for horizontal motions are summarised in Fig. 5. where zones of equal intensity are identified by K values. These values range from 0.1 to 100 corresponding to the thresholds for imperceptible and intolerable vibrations respectively.

Law et al (1980) stayed on the top floor of the ten-storey steel-frame experimental building in Hong Kong (sect 5. ) during typhoon winds. They found that when the wind speed was about 15 m/s, and the corresponding root-mean-square deflection of the building was 2 mm, the conditions were such as to induce fear. This was of two-fold origin: (i) fear that the windows might be broken and (ii) that the building might collapse. The measured frequency was 0.87 Hz and with a Dieckmann K-value of 4.3. The degree of fear in this case was certainly greater than that experienced in machine-induced factory vibrations with a higher value of K. At a speed of 25 m/s and a root-mean-square deflection of 3.6 mm the Dieckmann K-value rose to 8, and the state of fear became intolerable.

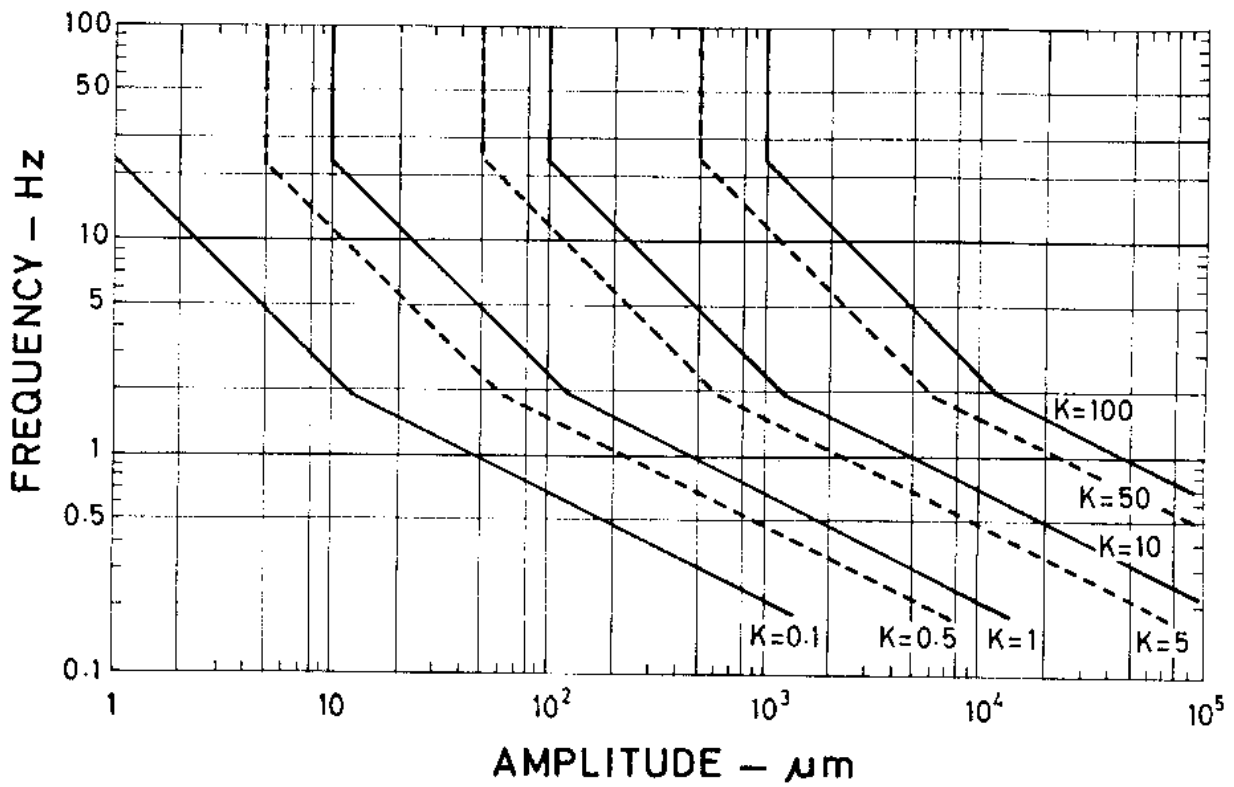


Fig. 5. Human sensitivity to horizontal vibrations expressed in Dieckmann's K values (After Lam et al 1980).

The noise from wind was alone sufficient to induce fear in persons standing on the ground floor. This experience indicates that wind noise in high rise buildings causes discomfort additional to that arising from vibrations of the main structures. Figures for noise levels generally in winds of typhoon force cannot be given as they depend on the number and type of obstacles - trees, wires, poles, buildings etc. - in the locality. The frightening noise caused by the impact of raindrops on windows is additional to that due to wind alone.

People exposed to the full force of winds of about 60 m/s or more tend to lose their clothing, for this reason most bodies found after the passage of severe tropical cyclones are nude or nearly so. During the passage of severe tropical cyclones people resident on atolls and low-lying coastal areas have had to climb and hang on to trees to avoid being carried away by surge or waves. Their exposed backs may then be scoured by driven rain and sea spray until they ~~were~~<sup>were</sup> raw and blistered, like a burn. The condition can also be due to the "sand blasting" by wind-borne gravel and sand. The same processes have stripped paint off ships and cars or "frosted" their windows.

It is surprising to many people to learn that humans exposed to severe typhoon conditions suffer from cold and shiver although the air temperature at the time may be 25°C or more. It has been established, for a variety of climatic conditions, that the sensation of "cold" derives mainly from wind speed, temperature is the least effective factor with long and short-wave radiation fluxes taking an intermediate position (Landsberg, 1972). In the heavily clouded eye-wall region of tropical cyclones there is little penetration of solar radiation and body heat is carried off at a great rate by the hurricane force winds. The rate of heat loss is termed "cooling power" and there is a large number of formulae to express this heat loss H in terms of the ambient temperature t and the wind speed v. Most equations take the form

$$H = (a + bv^c) (t_k - t). \quad \text{-- (5.1)}$$

where t is the air temperature and  $t_k$  is the normal skin temperature (33°C) or the average body temperature (usually taken as 36.5°C) and a, b and c are constants with the latter having a value between 0.5 and one. These

relationships have not been verified in typhoon conditions but the following formula - which is typical - has been verified for winds up to 16 m/s.

$$H = (0.23 + 0.47 \cdot v^{0.52}) (36.5 - t) \quad \text{mcal/cm}^2/\text{s} \quad \text{-- (5. )}$$

Table 6 shows that in a typhoon  $t$  is about  $26^\circ\text{C}$  and if  $v$  is taken as 60 m/s the heat loss would be  $44 \text{ mcal/cm}^2/\text{s}$ . In SI units this is equivalent to  $1842 \text{ W/m}^2$  (the factor is 41.87).

Equation (5. ) is for dry conditions, if the body is wet there will be additional cooling due to evaporation of water - the wet-bulb effect. However this will be countered, to some degree, by the prevailing high relative humidity and heavy rain which, from Table 6. , has a temperature of about  $25^\circ\text{C}$ . The heat loss  $H'$  from a wet body is given (Landsberg 1972) by the equation

$$H' = (0.37 + 0.51 \cdot v^{0.63}) (36.5 - t') \quad \text{mcal/cm}^2/\text{s} \quad \text{-- (5. )}$$

where  $t'$  is the wet-bulb temperature usually near  $24.8^\circ\text{C}$  (see Table 6. ). A wind of 60 m/s would then cause a cooling effect of  $83 \text{ mcal/cm}^3/\text{s}$ . Heat losses or cooling powers are usually related to some human sensation scale in which losses of more than  $32 \text{ mcal/cm}^2/\text{s}$  equate to the feelings "bitterly cold" or "extreme cold" (Landsberg 1972). Equation (5. ) indicates that when the wet-bulb temperature is  $24.8^\circ\text{C}$  the  $32 \text{ mcal/cm}^2/\text{s}$  criterion is attained at a wind speed as low as 11 m/s. Although equations (5. ) and (5. ) have not been verified in extreme typhoon conditions they do indicate that severe wind chill will occur at these times. Precise cooling rates have yet to be established.

The calculations of this section indicate that it is not necessary to be exposed to the full force of the winds to feel bitterly cold in a tropical cyclone. This is vividly highlighted in the account of cyclone Tracy 1974 at Darwin as given by Keith Cole in his book

"Winds of Fury" (Cole 1977). "After scrambling inside the store we took up our position behind the door, leaning against it in case it should be blown open. We were bitterly cold, as we were still in our night clothes. Fortunately Merle had put on a thick dressing gown and I had a blanket draped around me. We were drenched to the skin, but the wet wool afforded some warmth." Also, in the cryptic report of a medical officer "3:00 a.m. shed collapsed but all sheltered on one lawn mower with "deep freeze" on one side and 3-in. wall on the other. 6:00 a.m. cold, shivering, all soaked, all only in flimsy pyjamas."

Fletcher R D, Smith JR and Bundgaard R. C 1961  
Superior Photographic Reconnaissance of  
Tropical Cyclones. Weatherwise ~~14~~ 14, 103-109.

REFERENCES

Bell G.S. 1961 Surface winds in H-V - (1961) Proc U.S./Asian Weather Symposium: USAF, Air Weather Service

Frost, R. 1966. The relation between Beaufort Force wind speed and wave height. Met. Off., Scientific Paper No.25.

---

Gold, E. 1936. Wind in Britain. Quart. J. R. Met. Soc. 62, 167.

Hawkins, H.F. and Imbembo, S.M. 1976. The structure of a small, intense hurricane - Inez 1966. Mon. Wea. Rev. 104, p 418.

---

Ishizaki, H. 1972. On the large deflections of rectangular glass panes under uniform pressure. Bull. Bisaster. Prev. Res. Inst. Kyoto University, 22, 1.

---

Izumi, Y. and Barad, M.L. 1970. Wind speeds as measured by cup and sonic anemometers and influenced by tower structure. J. Appl. Met. 9, 851-856.

---

Küppen, W. 1898. Arch Seewarte, Hamburg, 21, 5.

---

MacCreedy, P.B. 1966. Mean wind speed measurements in turbulence. J. Appl. Met. 5, 219-225.

Mazzarella, D.A. 1972. An inventory of specifications  
for wind measuring instruments.  
Bull. Amer. Met. Soc. 53,860-871.

---

Meteorological Office 1956. "Handbook of  
Meteorological Instruments"  
H.M.S.O. London.

---

Saffir, H.S. 1977. Design and construction  
requirements for hurricane - resistant  
construction. A.S.C.E. Spring Convention  
preprint 2830.

---

Sanuki, M. 1952. A new development of the  
theoretical and experimental  
treatment of the lag of Dines  
pressure tube exposed in  
fluctuating winds. Papers in  
Met. and Geophys. 3, 115.

---

Simpson, G.C. 1906. Report of Dir. of Met. Off.,  
London, No. 180.

---

Simpson, G.C. 1926. The velocity equivalents of  
the Beaufort Scale. Prof. Notes,  
Met. Off., London, No.44.

Simpson, R.H., Sugg, A.L. and Staff, 1970.  
The Atlantic Hurricane Season of 1969.  
M.W.R., 98, 293.

Wu, J. 1969. Wind stress and surface roughness at  
air-sea interface. J. Geophys. Res. ,  
74, p.444